2 Tyres and wheels

2.1 Tyre requirements

The tyres are crucial functional elements for the transmission of longitudinal, lateral and vertical forces between the vehicle and road. The tyre properties should be as constant as possible and hence predictable by the driver. As well as their static and dynamic force transmission properties, the requirements described below – depending on the intended use of the vehicle – are also to be satisfied.

As tyres significantly affect the handling properties of vehicles, the properties of original tyres – the tyres with which the vehicle is supplied to the customer – are specified by the vehicle manufacturers in conjunction with the tyre manufacturers. However, spare tyres usually differ from the original tyres, despite their similar designation; hence handling characteristics can change. Individual vehicle manufacturers have therefore decided to identify tyres produced in accordance with their specifications by means of a symbol on the sidewall of the tyre or to sell tyres which meet the specifications of original tyres at their manufacturing branches.

2.1.1 Interchangeability

All tyres and rims are standardized to guarantee interchangeability, i.e. to guarantee the possibility of using tyres from different manufacturers but with the same designation on one vehicle and to restrict the variety of tyre types worldwide.

Within Europe, standardization is carried out by the European Tyre and Rim Technical Organization or ETRTO, which specifies the following:

- tyre and rim dimensions;
- the code for tyre type and size;
- the load index and speed symbol.

Passenger car tyres are governed by UNO regulation ECE-R 30, commercial vehicles by R 54, spare wheels by R 64, and type approval of tyres on the vehicle by EC directive 92/23/EC.

In the USA the Department of Transportation (or DOT, see item 9 in Fig. 2.18) is responsible for the safety standards. The standards relevant here are:

Standard 109	Passenger cars
Standard 119	Motor vehicles other than passenger cars.

The Tire and Rim Association, or TRA for short, is responsible for standardization.

In Australia, binding information is published by the Federal Office of Road Safety, Australian Motor Vehicle Certification Board.

ARD 23	Australian Design Rule 23/01: Passenger car tyres

is the applicable standard.

In Germany the DIN Standards (Deutsches Institut für Normung) and the WdK Guidelines (Wirtschaftsverband der Deutschen Kautschukindustrie Postfach 900360, D-60443, Frankfurt am Main) are responsible for specifying tyre data. All bodies recognize the publications of these two organizations.

At the international level, the ISO (International Organization for Standardization) also works in the field of tyre standardization and ISO Standards are translated into many languages.

2.1.2 Passenger car requirements

The requirements for tyres on passenger cars and light commercial vehicles can be subdivided into the following six groups:

- driving safety
- handling
- comfort
- service life
- economy
- environmental compatibility.

To ensure driving safety it is essential that the tyre sits firmly on the rim. This is achieved by a special tyre bead design (tyre foot) and the safety rim, which is the only type of rim in use today (Figs 2.5 and 2.21). Not only is as great a degree of tyre-on-rim retention as possible required, but the tyre must also be hermetically sealed; on the tubeless tyre this is the function of the inner lining. Its job is to prevent air escaping from the tyre, i.e. it stops the tyre from losing pressure. However, this pressure reduces by around 25–30% per year, which shows how important it is to check the tyre pressure regularly.

In order to guarantee driving safety, the aim is also to ensure that tyres are as insensitive to overloading and as puncture-proof as possible and that they have emergency running properties which make it possible for the driver to bring the vehicle safely to a halt in case of tyre failure.

Handling characteristics include the properties:

- high coefficients of friction in all operating conditions;
- steady build-up of lateral forces without sudden changes;
- good cornering stability;
- direct and immediate response to steering movements;
- guarantee requirement of sustained maximum speed;
- small fluctuations in wheel load.

Riding comfort includes the characteristics:

- good suspension and damping properties (little rolling hardness);
- high smoothness as a result of low radial tyre run-out and imbalances;
- little steering effort required during parking and driving;
- low running noise.

Durability refers to:

- long-term durability
- high-speed stability.

Both are tested on drum test stands and on the road.

Economic efficiency is essentially determined by the following:

- purchase cost;
- mileage (including the possibility of profile regrooving in the case of lorry tyres);
- wear (Fig. 3.46);
- rolling resistance;
- the necessary volume, which determines
- the amount of room required in the wheel houses and spare-wheel well;
- load rating.

Of increasing importance is environmental compatibility, which includes:

- tyre noise;
- raw material and energy consumption during manufacture and disposal;
- possibility of complete remoulding inherent in the construction.

The importance of

- tyre design, profile design and the 'radius–width appearance' must not be neglected either.

Further details are available in Refs [4], [6], [7] and [9].

2.1.3 Commercial vehicle requirements

In principle, the same requirements apply for commercial vehicles as for passenger cars, although the priority of the individual groups changes. After safety, economy is the main consideration for commercial vehicle tyres. The following properties are desirable:

- high mileage and even wear pattern
- low rolling resistance
- good traction
- low tyre weight
- ability to take chains
- remoulding/retreading possibilities.

Compared with passenger car tyres, the rolling resistance of commercial vehicle tyres has a greater influence on fuel consumption (20–30%) and is therefore an important point (Fig. 2.32).

2.2 Tyre designs

2.2.1 Diagonal ply tyres

In industrialized countries, cross-ply tyres are no longer used on passenger cars, either as original tyres or as replacement tyres, unlike areas with very poor roads where the less vulnerable sidewall has certain advantages. The same is true of commercial vehicles and vehicles that tow trailers, and here too radial tyres have swept the board because of their many advantages. Nowadays, cross-ply tyres are used only for:

- temporary use (emergency) spare tyres for passenger cars (due to the low durability requirements at speeds up to 80 or 100 km h^{-1});
- motor cycles (due to the inclination of the wheels against the lateral force);
- racing cars (due to the lower moment of inertia);
- agricultural vehicles (which do not reach high speeds).

Cross-ply tyres consist of the substructure (also known as the tyre carcass, Fig. 2.1) which, as the 'supporting framework' has at least two layers of rubberized cord fibres, which have a zenith or bias angle ξ of between 20° and 40° to the centre plane of the tyre (Fig. 2.2). Rayon (an artificial silk cord), nylon or even steel cord may be used, depending on the strength requirements. At the tyre feet the ends of the layers are wrapped around the core of the tyre bead on both sides; two wire rings, together with the folded ends of the plies, form the bead. This represents the frictional connection to the rim. The bead must thus provide the permanent seat and transfer drive-off and braking moments to the tyre. On tubeless tyres it must also provide the airtight seal.

The running tread, which is applied to the outer diameter of the substructure,

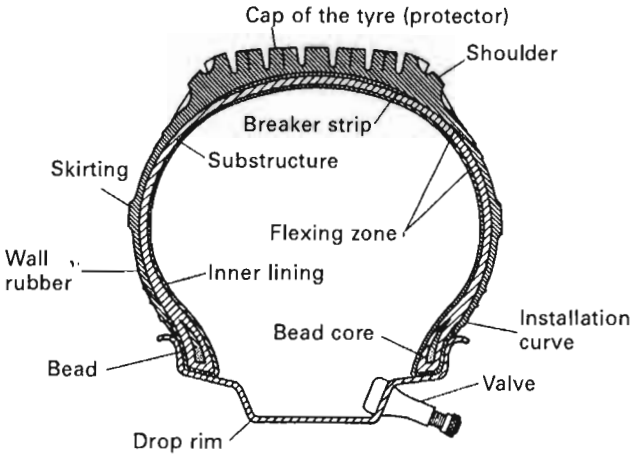

Fig. 2.1 Design of a diagonal ply tubeless car tyre with a normal drop rim and pressed-in inflating valve (see also Fig. 2.6).

Fig. 2.2 The diagonal ply tyre has crossed-bias layers; the zenith angle ξ was 30° to 40° for passenger cars. The 4 PR design should have two layers in each direction. Smaller angles ξ can be found in racing cars. Rolling resistance, lateral and suspension stiffness are significantly determined by the zenith angle.

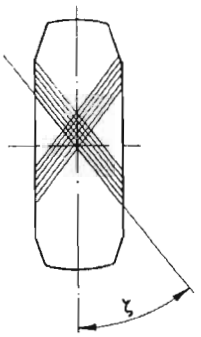

provides the contact to the road and is profiled. Some tyres also have an intermediate structure over the carcass as reinforcement.

At the side, the running tread blends into the shoulder, which connects to the sidewall (also known as the side rubber), and is a layer that protects the substructure. This layer and the shoulders consist of different rubber blends from the running tread because they are barely subjected to wear; they are simply deformed when the tyre rolls. This is known as flexing. Protective mouldings on the sides are designed to prevent the tyre from being damaged through contact with kerbstones. There are also GG grooves, which make it possible to see that the tyre is seated properly on the rim flange.

Cross-ply design and maximum authorized speed are indicated in the tyre marking by a dash (or a letter, Fig. 2.12) between the letters for width and rim

diameter (both in inches) and a 'PR' (ply rating) suffix. This ply rating refers to the carcass strength and simply indicates the possible number of plies (Fig. 2.5). The marking convention is:

5.60-15/4 PR	(VW rear-engine passenger car, tyres authorized up to 150 km h^{-1})
7.00-14/8 PR	(VW Transporter, tyres authorized up to 150 km h^{-1})
9.00-20/14 PR	(reinforced design for a commercial vehicle)

and on the temporary use spare wheel of the VW Golf, which requires a tyre pressure of p_T = 4.2 bar and may only be driven at speeds up to 80 km h^{-1} (F symbol)

T 105/70 D 14 38 F

2.2.2 Radial ply tyres

The radial ply tyre consists of two bead cores joined together radially via the carcass (Fig. 2.3) – hence the name radial tyres. A belt of cords provides the necessary stiffness (Fig. 2.4), whereas the external part of the tyre consists of the tread and sidewall and the interior of the inner lining, which ensures the tyre is hermetically sealed (Figs 2.5 and 2.1). In passenger car tyres, the carcass is made of rayon or nylon, the belt of steel cord or a combination of steel, rayon or nylon cord, and the core exclusively of steel. Due to the predominance of steel as the material for the belt, these tyres are also known as 'steel radial tyres'. The materials used are indicated on the sidewall (Fig. 2.18, points 7 and

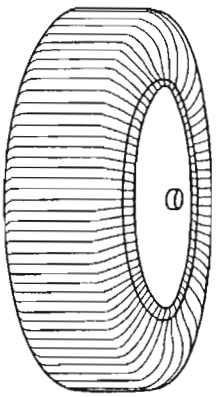

Fig. 2.3 Substructure of a radial tyre. The threads have a bias angle between 88° and 90°.

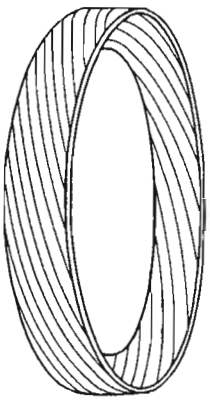

Fig. 2.4 The belt of the radial tyre sits on the substructure. The threads are at angles of between 15° and 25° to the plane of the tyre centre.

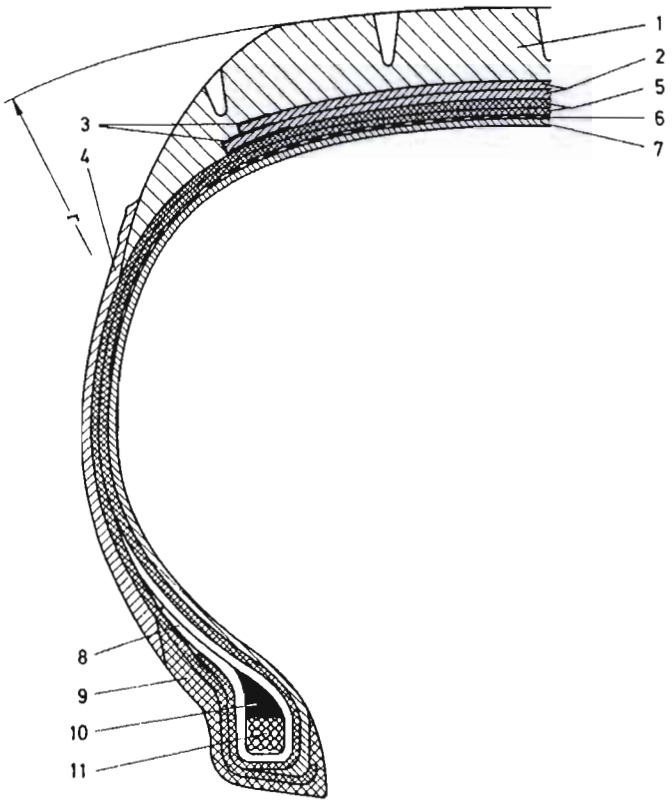

Fig. 2.5 Radial design passenger car tyres in speed category T (Fig. 2.12); the number of layers and the materials are indicated on the sidewall (see Fig. 2.18). The components are: 1 running tread; 2 steel belt; 3 edge protection for the belt, made of rayon or nylon; 4 sidewall; 5 substructure with two layers; 6 cap; 7 inner lining; 8 flipper; 9 bead profile; 10 core profile; 11 bead core.

8). In commercial vehicle designs this is particularly important and the carcass may also consist of steel.

The stiff belt causes longitudinal oscillation, which has to be kept away from the body by wheel suspensions with a defined longitudinal compliance, otherwise this would cause an unpleasant droning noise in the body, when on cobbles and poor road surfaces at speeds of less than 80 km h^{-1} (see Sections 3.6.5.2 and 5.1.2). The only other disadvantage is the greater susceptibility of the thinner sidewalls of the tyres to damage compared with diagonal ply tyres. The advantages over cross-ply tyres, which are especially important for today's passenger cars and commercial vehicles, are:

- significantly higher mileage
- greater load capacity at lower component weight

- lower rolling resistance
- better aquaplaning properties
- better wet-braking behaviour
- transferable, greater lateral forces at the same tyre pressure
- greater ride comfort when travelling at high speeds on motorways and trunk roads.

2.2.3 Tubeless or tubed

In passenger cars, the tubeless tyre has almost completely ousted the tubed tyre. The main reasons are that the tubeless tyre is

- easier and faster to fit
- the inner lining is able to self-seal small incisions in the tyre.

In tubeless tyres the inner lining performs the function of the tube, i.e. it prevents air escaping from the tyre. As it forms a unit with the carcass and (unlike the tube) is not under tensional stress, if the tyre is damaged the incision does not increase in size, rapidly causing loss of pressure and failure of the tyre. The use of tubeless tyres is linked to two conditions:

- safety contour on the rim (Fig. 2.21)
- its air-tightness.

Because this is not yet guaranteed worldwide, tubed tyres continue to be fitted in some countries. When choosing the tube, attention should be paid to ensuring the correct type for the tyre. If the tube is too big it will crease, and if it is too small it will be overstretched, both of which reduce durability. In order to avoid confusion, the tyres carry the following marking on the sidewall:

tubeless (Fig. 2.18, point 3)
tubed or tube type.

Valves are needed for inflating the tyre and maintaining the required pressure. Various designs are available for tubeless and tubed tyres (Figs 2.6 and 2.7). The most widely used valve is the so-called 'snap-in valve'. It comprises a metal foot valve body vulcanized into a rubber sheath, which provides the seal in the rim hole (Fig. 2.20). The functionality is achieved by a valve insert, while a cap closes the valve and protects it against ingress of dirt.

At high speeds, the valve can be subjected to bending stress and loss of air can occur. Hub caps and support areas on alloy wheels can help to alleviate this (see Fig. 2.24 and Section 7.2 in Ref. [4]).

2.2.4 Height-to-width ratio

The height-to-width ratio H/W – also known as the 'profile' (high or low) – influences the tyre properties and affects how much space the wheel requires

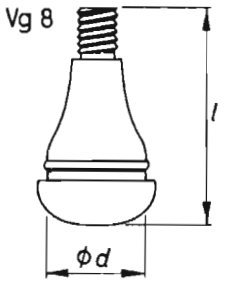

DIN	*l*	Diameter *d*
43 GS 11.5	43	15.2
43 GS 16	43	19.5

Fig. 2.6 Snap-in rubber valve for tubeless tyres, can be used on rims with the standard valve holes of 11.5 mm and 16 mm diameter. The numerical value 43 gives the total length in mm (dimension *l*). There is also the longer 49 GS 11.5 design.

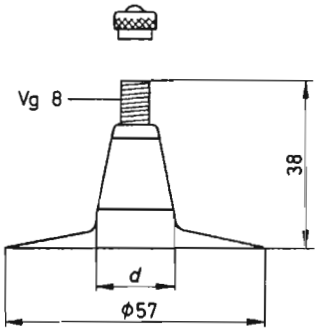

Valve specification	*d*
38/11.5	11.7
38/16	16.5

Fig. 2.7 Rubber valve vulcanized onto tubes. Designations are 38/11.5 or 38/16.

Fig. 2.8 Tyre sizes and associated rims used on the VW Golf III. All tyres fit flush up to the outer edge of the wing (wheel house outer panel) K. To achieve this, differing wheel offsets (depth of dishing) *e* are used on disc-type wheels (Fig. 2.23) with the advantage of a more negative rolling radius r_r on wider tyres (Fig. 3.102). A disadvantage then is that snow chains can no longer be fitted and steering sensitivity changes very slightly.

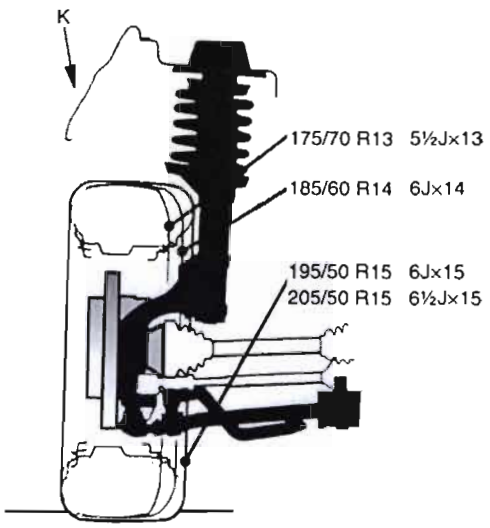

(Fig. 2.8). As shown in Fig. 2.9, the narrower tyres with a H/W ratio = 0.70 have a reduced tread and therefore good aquaplaning behaviour (Fig. 2.35). Wide designs make it possible to have a larger diameter rim and bigger brake discs (Fig. 2.10) and can also transmit higher lateral and longitudinal forces.

W is the cross-sectional width of the new tyre (Fig. 2.11); the height H can easily be calculated from the rim diameter given in inches and the outside diameter of the tyre OD_T. The values OD_T and W are to be taken from the new tyre

Fig. 2.9 If they have the same outside diameter and load capacity the four tyre sizes used on medium-sized passenger cars are interchangeable. The series 65, 55 and 45 wide tyres each allow a 1″ larger rim (and therefore larger brake discs). The different widths and lengths of the tyre contact patch, known as 'tyre print', are clearly shown (Fig. 3.119), as are the different designs of the standard road profile and the asymmetric design of the sports profile (see also Section 2.2.10). The 65 series is intended for commercial vehicles, and the 60, 55 and 45 series for sports cars. (Illustration: Continental; see also Fig. 2.19.)

Fig. 2.10 The flatter the tyre, i.e. the larger the rim diameter d (Fig. 2.11) in comparison with the outside diameter OD_T, the larger the brake discs or drums that can be accommodated, with the advantage of a better braking capacity and less tendency to fade. An asymmetric well-base rim is favourable (Figs 1.8 and 2.11).

Wheel rim diameter in inches	12	13	14	15	16	17
Brake disc outer diameter in mm	221	256	278	308	330	360
Brake drum inner diameter in mm	200	230	250	280	300	325

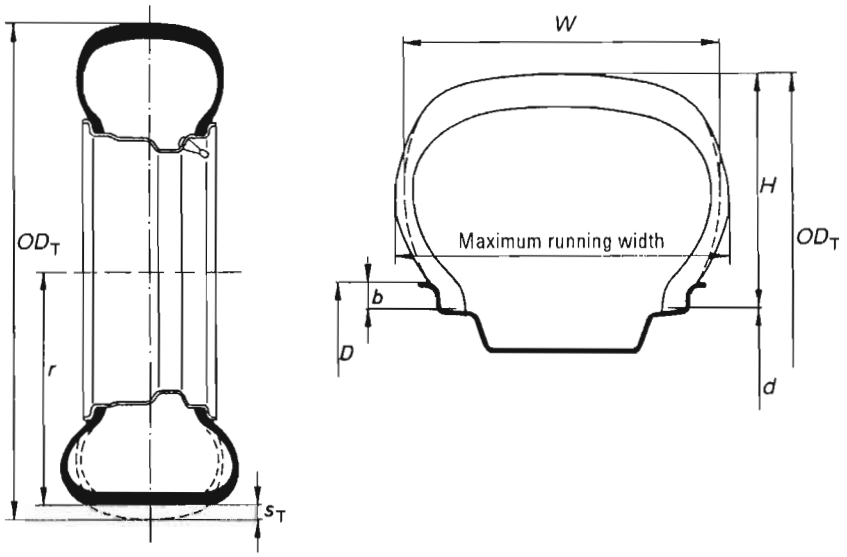

Fig. 2.11 Tyre dimensions specified in standards and directives. B is the cross-section width of the new tyre; the tread moulding (as can be seen in Fig. 2.1) is not included in the dimension. For clearances, the maximum running width with the respective rim must be taken into consideration, as should the snow chain contour for driven axles. The tyre radius, dependent on the speed, is designated r (see Section 2.2.8). Pictured on the left is an asymmetrical well-base rim, which creates more space for the brake caliper and allows a larger brake disc (Fig. 2.10).

mounted onto a measuring rim at a measuring tyre pressure of 1.8 bar or 2.3 bar on V-, W- or ZR tyres, Fig. 2.15):

$$H = 0.5\ (OD_T - d) \tag{2.1}$$

$$1'' = 1\ \text{in} = 25.4\ \text{mm} \tag{2.1a}$$

The 175/65 R 14 82 H tyre mounted on the measuring rim 5J × 14 can be taken as an example:

OD_T = 584 mm, d = 14 × 25.4 = 356 mm and W = 177 mm

$H/W = [0.5 \times (OD_T - d)]/W = 114/177 = 0.644$

The cross-section ratio is rounded to two digits and given as a percentage. We talk of 'series', and here the ratio profile is 65% as shown in the tyre marking – in other words it is a 65 series tyre. A wider rim, e.g. 6J × 14 would give a smaller percentage.

2.2.5 Tyre dimensions and markings

2.2.5.1 Designations for passenger cars up to 270 km h^{-1}

The ETRTO standards manual of the European Tire and Rim Technical Organization includes all tyres for passenger cars and delivery vehicles up to 270 km h^{-1} and specifies the following data:

- tyre width in mm
- height-to-width ratio as a percentage
- code for tyre design
- rim diameter in inches or mm
- operational identification, comprising load index; LI (carrying capacity index) and speed symbol GSY.

The following applies to the type shown in Fig. 2.15:

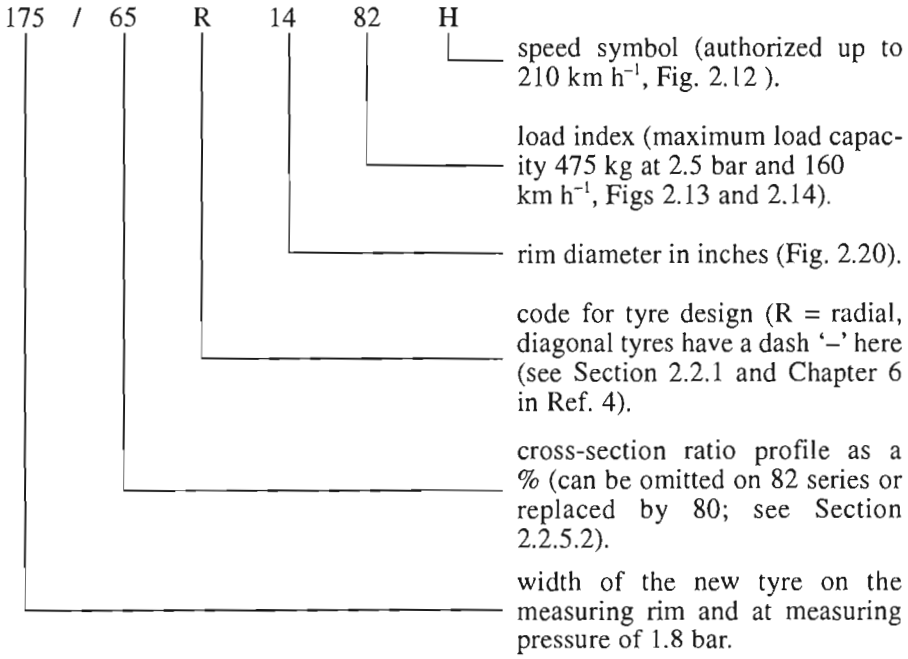

Fig. 2.12 Standardized speed categories for radial tyres, expressed by means of a speed symbol and – in the case of discontinued sizes – by means of the former speed marking. Sizes marked VR or ZR may be used up to maximum speeds specified by the tyre manufacturer. The symbols F and M are intended for emergency (temporary use) spare wheels (see Chapter 6 in Ref. [5]).

v_{max} *in km/h*$^{-1}$	*Speed symbol*	*Identification*
80	F	
130	M	
150	P	
160	Q	
170	R	
180	S	
190	T	
210	H	
240	V	
270	W	
300	Y	
over 210	—	VR
over 240	—	ZR (old system)

The old markings can still be found on individual tyres:

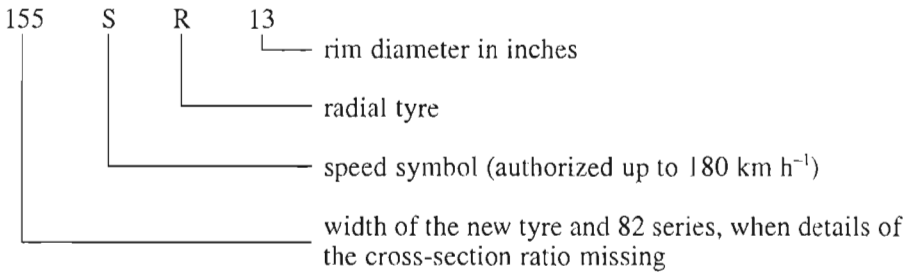

2.2.5.2 Designations of US tyres and discontinued sizes for passenger cars

Tyres manufactured in the USA and other non-European countries may also bear a 'P' for passenger car (see Fig. 2.17) and a reference to the cross-section ratio:

P 155/80 R 13 79 S

The old system applied up until 1992 for tyres which were authorized for speeds of over $V = 210$ km h^{-1} (or 240 km h^{-1}, Fig. 2.12); the size used by Porsche on the 928 S can be used as an example:

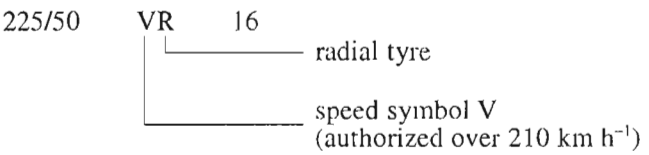

Fig. 2.13 Load capacity/air pressure category specified in the directives. The load capacity on the left – also known as 'load index' (LI) – applies for all passenger cars up to the speed symbol W; they relate to the minimum load capacity values up to 160 km h^{-1} at tyre pressure 2.5 bar (see Section 2.2.6). Further criteria, such as maximum speed, handling etc., are important for the tyre pressures to be used on the vehicle. For LI values above 100, further load increases are in 25 kg increments:

LI = 101 corresponds to 825 kg,
LI = 102 corresponds to 850 kg etc. to
LI = 108 corresponds to 1000 kg.

Load index	*Wheel load capacity in kg with tyre pressure measured in bars* 1.5	1.6	1.7	1.8	1.9	2.0	2.1	2.2	2.3	2.4	2.5
69	215	225	240	250	260	270	285	295	305	315	325
70	225	235	245	260	270	280	290	300	315	325	335
71	230	240	255	265	275	290	300	310	325	335	345
72	235	250	260	275	285	295	310	320	330	345	355
73	245	255	270	280	295	305	315	330	340	355	365
74	250	260	275	290	300	315	325	340	350	365	375
75	255	270	285	300	310	325	335	350	360	375	387
76	265	280	295	310	320	335	350	360	375	385	400
77	275	290	305	315	330	345	360	370	385	400	412
78	280	295	310	325	340	355	370	385	400	410	425
79	290	305	320	335	350	365	380	395	410	425	437
80	300	315	330	345	360	375	390	405	420	435	450
81	305	325	340	355	370	385	400	415	430	445	462
82	315	330	350	365	380	395	415	430	445	460	475
83	325	340	360	375	390	405	425	440	455	470	487
84	330	350	365	385	400	420	435	450	470	485	500
85	340	360	380	395	415	430	450	465	480	500	515
86	350	370	390	410	425	445	460	480	495	515	530
87	360	380	400	420	440	455	475	490	510	525	545
88	370	390	410	430	450	470	485	505	525	540	560
89	385	405	425	445	465	485	505	525	545	560	580
90	400	420	440	460	480	500	520	540	560	580	600
91	410	430	450	475	495	515	535	555	575	595	615
92	420	440	465	485	505	525	550	570	590	610	630
93	430	455	475	500	520	545	565	585	610	630	650
94	445	470	490	515	540	560	585	605	625	650	670
95	460	485	505	530	555	575	600	625	645	670	690
96	470	495	520	545	570	595	620	640	665	685	710
97	485	510	535	560	585	610	635	660	685	705	730
98	500	525	550	575	600	625	650	675	700	725	750
99	515	540	570	595	620	650	675	700	725	750	775
100	530	560	590	615	640	670	695	720	750	775	800

Fig. 2.14 The tyre load capacity shown in the ETRTO standards manual in the form of the load index LI is valid for V tyres up to vehicle speeds of 210 km h^{-1}; for W tyres up to 240 km h^{-1} and for Y tyres up to 270 km h^{-1}. At higher speeds, lower percentages of the load capacity must be incurred; for VR and ZR tyres, which are no longer made, these values were determined by vehicle and tyre manufacturers.

	Tyre load capacity (%)		
Top speed of car	*Speed symbol*		
(km h^{-1})	*V*	*W*	*Y Tyres*
210	100	100	100
220	97	100	100
230	94	100	100
240	91	100	100
250	–	95	100
260	–	90	100
270	–	85	100
280	–	–	95
290	–	–	90
300	–	–	85

The following should be noted for VR tyres:

- over 210 km h^{-1} and up to 220 km h inclusive, the load may only be 90% of the otherwise authorized value;
- over 220 km h^{-1} the carrying capacity reduces by at least 5% per 10 km h^{-1} speed increment.

2.2.5.3 Designation of light commercial vehicle tyres

Tyres for light commercial vehicles have a reinforced substructure compared with those for passenger cars (Fig. 2.5), so they can take higher pressures, which means they have a higher load capacity. The suffix 'C' followed by information on the carcass strength (6, 8 or 10 PR) used to indicate suitability for use on light commercial vehicles, or the word 'reinforced' simply appeared at the end of the marking. The current marking (as for passenger cars) retains the speed symbol as well as the load index which, behind the slash, gives the reduced load capacity on twin tyres (Fig. 3.4). Compared with the previous marking, the new system is as follows:

Former	*Current*
–	205/65 R 15 98 S (Fig. 2.15)
185 SR 14	185 R 14 90 S
185 SR 14 reinforced	185 R 14 94 R
185 R 14 C 6 PR	185 R 14 99/97 M
185 R 14 C 8 PR	185 R 14 102/100 M

The 185 R 14 tyre is a passenger car size which is also fitted to light commercial vehicles.

2.2.5.4 Tyre dimensions

Figure 2.15 shows the important data for determining tyre size:

- size marking;
- authorized rims and measuring rim;
- tyre dimensions: width and outside diameter new and maximum during running;
- static rolling radius (Fig. 2.11);
- rolling circumference (at 60 km h^{-1}, Fig 2.16, see also Section 2.2.8);
- load capacity coefficient (load index LI, Fig. 2.13);
- tyre load capacity at 2.5 bar and up to 160 km h^{-1} (see Section 2.2.6).

2.2.6 Tyre load capacities and inflation pressures

The authorized axle loads $m_{V,f,max}$ and $m_{V,r,max}$ (see Section 5.3.5), and the maximum speed v_{max} of the vehicle, determine the minimum tyre pressure. However, the required tyre pressure may be higher to achieve optimum vehicle handling (see also Section 2.10.3.5 and Fig. 2.44).

2.2.6.1 Tyre load capacity designation

The load capacities indicated in the load index (item 6, Fig. 2.18) are the maximum loads per tyre permitted for all tyres up to the speed symbol 'H'. They are valid up to speeds of 210 km h^{-1} for tyres marked 'V' and up to 240 km h^{-1} for those marked 'R' 'W' or 'ZR'. For vehicles with a higher top speed, the load capacity has to be reduced accordingly.

Consequently, for tyres with speed symbol 'V', at a maximum speed of 240 km h^{-1} the load capacity is only 91% of the limit value (Fig. 2.14). Tyres designated 'W' on the sidewall are only authorized up to 85% at 270 km h^{-1}. In both cases the load capacity values between 210 km h^{-1} ('V' tyre) and 240 km h^{-1} ('W' tyre) and the maximum speed must be determined by linear interpolation.

For higher speeds (ZR tyres), the interpolation applies to the 240–270 km h^{-1} speed range. At higher speeds, the load capacity as well as the inflating pressure will be agreed between the car and tyre manufacturers. However, this approval does not necessarily apply to tyres which are specially produced for the US market and which bear the additional marking 'P' (Fig. 2.17 and Section 2.2.5.2).

2.2.6.2 Tyre pressure determination

For tyres with speed symbols 'R' to 'V' and standard road tyres the minimum pressures set out in the tables and corresponding with load capacities are valid up to 160 km h^{-1} (see Fig. 2.15 and Section 2.1.1).

Special operating conditions, the design of the vehicle or wheel suspension and expected handling properties can all be reasons for higher pressure specification by the vehicle manufacturer.

Further, for speeds up to 210 km h^{-1} the linear increase of basic pressure has to be by 0.3 bar (i.e. by 0.1 bar per Δv = 17 km h^{-1}; see also end of Section 2.84) and at speeds above 210 km h^{-1} the tyre load capacity has to be reduced

Fig. 2.15 Radial 65 series tyres, sizes, new and running dimensions, authorized rims and load capacity values (related to maximum 160 km h^{-1} and 2.5 bar); the necessary increase in pressures at higher speeds can be taken from Section 2.2.6. The tyre dimensions apply to tyres of a normal and increased load capacity design (see Section 2.2.5.3) and to all speed symbols and the speed marking ZR.

	Dimensions of new tyre					*Manufacturer's measurements*				
Tyre size	*Measuring rim*	*Width of cross-section*	*Outer diameter*	*Permissible rims according to DIN 7817 and DIN 7824*	*Max. width*	*Max. outer diameter*[4]	*Static radius ±2.0%*	*Circum-ference +1.5% −2.5%*	*Load index (LI)*	*Wheel load capacity*[5]
155/65 R 13	4.50 B × 13	157	532	4.00 B × 13[1]	158	540	244	1625	73	365
				4.50 B × 13[1]	164					
				5.00 B × 13[1]	169					
				5.50 B × 13[1]	174					
155/65 R 14	4½ J × 14	157	558	4 J × 14[2]	158	566	257	1700	74	375
				4½ J × 14[2]	164					
				5 J × 14[2]	169					
				5½ J × 14[2]	174					
165/65 R 13	5.00 B × 13	170	544	4.50 B × 13[1]	171	533	248	1660	76	400
				5.00 B × 13[1]	176					
				5.50 B × 13[1]	182					
				6.00 B × 13[1,3]	187					
165/65 R 14	5 J × 14	170	570	4½ J × 14[2]	171	579	261	1740	78	425
				5 J × 14[2]	176					
				5½ J × 14[2]	182					
				6 J × 14	187					
175/65 R 13	5.00 B × 13	177	558	5.00 B × 13[1]	184	567	254	1700	80	450
				5.50 B × 13[1]	189					
				6.00 B × 13[1,3]	194					
175/65 R 14	5 J × 13	177	584	5 J × 14[2]	184	593	267	1780	82	475
				5½ J × 14[2]	189					
				6 J × 14	194					
175/65 R 15	5 J × 15	177	609	5 J × 15[2]	184	618	279	1855	83	487
				5½ J × 15[2]	189					
				6 J × 15	194					
185/65 R 13	5.50 B × 14	189	570	5.50 B × 13[1]	191	580	259	1740	84	500
				5.50 B × 13[1]	197					
				6.00 B × 13[1,3]	202					
				6½ J × 13	207					
185/65 R 14	5½ J × 14	189	596	5 J × 14	191	606	272	1820	86	530
				5½ J × 14	197					
				6 J × 14	202					
				6½ J × 14	207					

185/65 R 15	5½ J × 15	189	621	5 J × 15	191	631	284	1895	88	560
				5½ J × 15	197					
				6 J × 15	202					
				6½ J × 15	207					
195/65 R 14	6 J × 14	201	610	5½ J × 14	204	620	277	1860	89	580
				6 J × 14	209					
				6½ J × 14	215					
				7 J × 14	220					
195/65 R 15	6 J × 15	201	635	5½ J × 15	204	645	290	1935	91	615
				6 J × 15	209					
				6½ J × 15	215					
				7 J × 15	220					
205/65 R 14	6 J × 14	209	622	5½ J × 14	212	633	282	1895	91	615
				6 J × 14	217					
				6½ J × 14	222					
				7 J × 14	227					
				7½ J × 14	233					
205/65 R 15	6 J × 15	209	647	5½ J × 15	212	658	294	1975	94[6]	670
				6 J × 15	217					
				6½ J × 15	222					
				7 J × 15	227					
				7½ J × 15	233					
215/65 R 15	6½ J × 15	221	661	6 J × 15	225	672	300	2015	96[7]	710
				6½ J × 15	230					
				7 J × 15	235					
				7½ J × 15	240					
215/65 R 16	6½ J × 16	221	686	6 J × 16	225	697	312	2090	98	750
				6½ J × 16	230					
				7 J × 16	235					
				7½ J × 16	240					
225/65 R 15	6½ J × 15	228	673	6 J × 15	232	685	304	2055	99	775
				6½ J × 15	237					
				7 J × 15	242					
				7½ J × 15	248					
				8 J × 15	253					

[1] Instead of wheel rims with the identification letter B, same-sized rims with the identification letter J may be used. For example 5½ J × 13 instead of 5.50 B × 13. (See Section 2.3.2.)
[2] Instead of wheel rims with the identification letter J, same-sized rims with the identification letter B may be used. For example 4.50 B × 14 instead of 4½ J × 14.
[3] The wheel rims without identification letters mentioned in the table are expected to be identified with DIN 7824 Part 1.
[4] The outer diameter of wheels with M & S – tread can be up to 1% bigger than the standard tread.
[5] Maximum in kg at 2.5 bar.
[6] Reinforced model, 750 kg at 3.0 bar (LI 98).
[7] Reinforced model, 800 kg at 3.0 bar (LI 100).

Fig. 2.16 Factor k_v, which expresses the speed dependence of the rolling circumference of passenger vehicle radial tyres above 60 km h^{-1} as a percentage. The permissible tolerances Δk_v have to be added (see Section 2.2.8), all taken from the German WDK Guideline 107, page 1.

v (km h^{-1})	60	90	120	150	180	210	240
Factor k_v (%)	–	+0.1	+0.2	+0.4	+0.7	+1.1	+1.6
Deviation Δk_v (%)	–	±0.1	±0.2	±0.4	±0.7	±1.1	±1.6

Fig. 2.17 ZR tyres manufactured specially for the American market and marked with a 'P' do not meet the European standard and are therefore not authorized here (photograph: Dunlop factory).

in accordance with item 2.2.6.1. If the tyre load is lower than the maximum load capacity, a lower additional safety pressure can be used in consultation with the tyre manufacturer.

For tyres with the speed symbol 'W', the pressures in Fig. 2.13 apply up to 190 km^{-1}. After this it has to be increased by 0.1 bar for every 10 km h^{-1} up to 240 km h^{-1}. For higher speeds, the load capacity must be reduced (see Section 2.2.6.1).

On vehicles, pressure should be tested on cold tyres, i.e. these must be adjusted to the ambient temperature. If the tyre pressure is set in a warm area in winter there will be an excessive pressure drop when the vehicle is taken outside.

On M & S winter tyres it has long been recommended that inflation pressures be increased by 0.2 bar compared with standard tyres. Newer brands of tyre no longer require this adjustment.

2.2.6.3 Influence of wheel camber

Wheel camber angles ε_W considerably influence tyre performance and service life. The camber angle should therefore not exceed 4° even in full wheel jounce condition. For angles above ±2° (see Section 3.5.1), the loadability of the tyres reduces at

$\varepsilon_W > 2°$ to 3° to 95%
$\varepsilon_W > 3°$ to 4° to 95%

Intermediate values have to be interpolated. Compensation can be achieved by increasing the inflation pressure. The values are as follows:

Camber angle	2°20′	2°40′	3°	3°20′	3°40′	4°
Pressure increase	2.1%	4.3%	6.6%	9.0%	11.5%	14.1%

Taking all the influences into account, such as top speed, wheel camber and axle load, the minimum tyre pressure required can be calculated for each tyre category (size and speed symbol). Formulas are shown in the 'WdK 99' guidelines from the Wirtschaftsverband der Deutschen Kautschukindustrie.

2.2.6.4 Tyre pressure limit values

Tyre pressure limit values should be adhered to. These values are

Q and T tyres	3.2 bar
H to W and ZR tyres	3.5 bar
M & S tyres (Q and T tyres)	3.5 bar

2.2.7 Tyre sidewall markings

All tyres used in Europe should be marked in accordance with the ETRTO standards (see Section 2.1.1).

In the USA, Japan and Australia, additional markings are required to indicate the design of the tyre and its characteristics. The characters must also bear the import sizes – the reason why these can be found on all tyres manufactured in Europe (Fig. 2.18).

2.2.8 Rolling circumference and driving speed

The driving speed is:

$$v = 0.006(1 - S_{X,W,a})\frac{C_{R,dyn} \times n_M}{i_D \times i_G} \text{ (km/h)} \qquad (2.1b)$$

This includes:

$S_{X,W,a}$	the absolute traction slip (Equation 2.4f)
$C_{R,dyn}$	the dynamic rolling circumference in m (Equation 2.1d)
n_M	the engine speed in rpm
i_D	the ratio in the axle drive (differential)
i_G	the ratio of the gear engaged (Equation 6.36)

The following can be assumed for slip $S_{X,W,a}$:

1st gear	0.08	4th gear	0.035
2nd gear	0.065	5th gear	0.02
3rd gear	0.05		

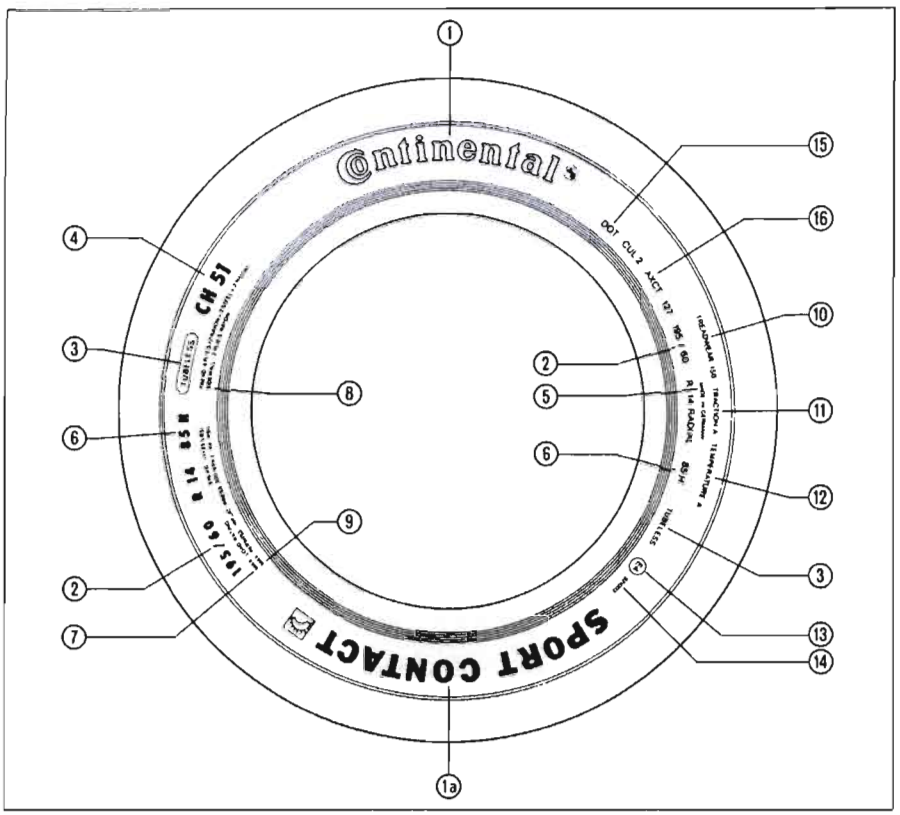

Fig. 2.18 Explanation of the marking on the sidewall of a tyre manufactured by Pneumatiques Kléber SA:

Legal and industry standard markings on the sidewalls of tyres according to:
FMVSS and CIR 104
UTQG (USA)
CSA Standard (Canada)
ADR 23B (Australia)
ECE–R30 (Europe)

1 Manufacturer (brand)
1a Product name
2 Size marking
195 = nominal tyre wideth in mm
60 = height–width ratio (60%)
radial type construction
14 rim diameter in inches
3 Tubeless
4 Trade code
5 Country of manufacture
6 Load capacity index (LI)
7 Maximum load capacity for the USA
8 Tread: under the tread are 6 plies carcass rayon, 2 plies steel belt, 2 plies nylon)
Sidewall: the substructure consists of 2 plies rayon
9 Maximum tyre pressure for the USA
10, 11, 12 USA: manufacturer's guarantee of compliance with the Uniform Tire Quality Grade (UTQG) which specifies: 10 tread wear: relative life expectancy compared with US-specific standard test values; 11 traction: A, B, C = braking performance on wet surfaces 12 temperature resistance: A, B or C = temperature resistance at higher test stand speeds; C fulfills the legal requirement in the USA
13 E 4 = tyre fullils the ECE R30 value requirements
4 = country in which approval was carried out
(4 = The Netherlands)
14 identity number according to ECE R-30
15 DOT = tyre fulfils the requirements according to FMVSS 109 (DOT = Department of Transportation)
16 Manufacturer's code:
CU = factory (Continental)
L2 = tyre size
AXCT = model
127 = date of manulacture: production week 12, 1987

According to DIN 75020 Part 5, the rolling circumference C_R given in the tyre tables relates to 60 km/h and operating pressure of 1.8 bar. At lower speeds it goes down to $C_{R,stat}$:

$$C_{R,stat} = r_{stat}\, 2\pi \tag{2.1c}$$

The values for r_{stat} are also given in the tables. At higher speeds, C_R increases due to the increasing centrifugal force. The dynamic rolling circumference $C_{R,dyn}$ at speeds over 60 km h^{-1} can be determined using the speed factor k_v. Figure 2.16 shows the details for k_v as a percentage, increasing by increments of 30 km h^{-1}. Intermediate values must be interpolated. The circumference would then be:

$$C_{R,dyn} = C_R\,(1 + 0.01 \times k_v)\ (\text{mm}) \tag{2.1d}$$

The dynamic rolling radius can be calculated from $C_{R,dyn}$ as

$$r_{dyn} = C_R/2\pi$$

or, at speeds of more than 60 km h^{-1},

$$r_{dyn} = C_{R,dyn}/2\pi \tag{2.2}$$

Taking as an example the tyre 175/65 R 14 82 H at v = 200 km h^{-1} (Fig. 2.15) gives

$$k_{v180} = 0.7\% \text{ and } k_{v210} = 1.1\%$$

and interpolation gives:

$$k_{v200} = 0.007 + 0.0027 = 0.0097$$
$$k_{v200} = 0.97\%$$

The rolling circumference C_R taken from Fig. 2.15, according to Equation 2.1d, gives

$$C_{R,dyn200} = 1780 \times (1 + 0.0097) = 1797 \text{ mm}$$

and thus the dynamic radius in accordance with Equation 2.2 is:

$$r_{dyn60} = 283 \text{ mm and } r_{dyn200} = 286 \text{ mm}$$

The outside diameter (construction measure) is

$$OD_T = 584 \text{ mm and thus } OD_T/2 = 292 \text{ mm}$$

a value which shows the extent to which the tyre becomes upright when the vehicle is being driven: r_{dyn} is only 9 mm or 6 mm less than $OD_T/2$. Chapter 3 of Ref. [3] gives further details.

2.2.9 Influence of the tyre on the speedometer

The speedometer is designed to show slightly more than, and under no circumstances less than, the actual speed. Tyres influence the degree of advance, whereby the following play a role:

- the degree of wear
- the tolerances of the rolling circumference
- the profile design
- associated slip.

The EC Council directive 75/443, in force since 1991, specifies an almost linear advance Δv,

$$+\Delta v \leqslant 0.1 \times v + 4 \text{ (km h}^{-1}\text{)} \qquad (2.2a)$$

On vehicles registered from 1991 onwards the values displayed may only be as follows:

Actual speed (km h^{-1})	30	60	120	180	240
Max displayed value (km h^{-1})	37	70	136	202	268

As Fig. 2.15 indicates, at 60 km h^{-1} the rolling circumference C_R has a tolerance range of $\Delta C_R = +1.5\%$ to -2.5%, and according to Fig. 2.16 with a speed factor of k_v, deviations of up to $\Delta k_v = \pm 1.6\%$ are possible. When related to the dynamic rolling circumference $C_{R,dyn}$ (Equation 2.1d), the following tolerance limits (rounded to the nearest figure) may prevail and result in the displayed values when only the minus tolerances are considered, and if the speedometer has the maximum authorized advance:

Actual speed (km h^{-1})	60	120	180	240
Possible overall tolerance (%)	+1.5	+1.7	+2.2	+3.1
	−2.5	−2.7	−3.2	−4.1
Max display value at minus tolerance (km h^{-1})	72	140	208	279

The slip should be added directly to this, which in direct gear amounts to around 2% (see equations 2.1b and 2.4f), in other words

$$S_{X,W,a} = 0.02$$

If the manufacturer fully utilizes the advance specified in Equation 2.2a, it is possible that although the speedometer indicates 140 km h^{-1}, the vehicle is only moving at 120 km h^{-1}. This occurs, in particular, when the tyres are worn:

3 mm wear gives an advance of around 1%

Fig. 2.19 Designs of Continental tyre. (Top) Summer tyre (tyre foot prints see Fig. 2.9) EcoContact EP (size 185/65 R14T) and Sport Contact (size 205/55 R16W). (Below) Winter tyre WinterContact TS760 (size 185/65 R14T) and WinterContact TS770 (size 235/60 R16H).

Tyres with an M & S winter profile can, however, have a 1% larger outside diameter so that the profile can be deeper (Fig. 2.15, note 5 and Fig. 2.19). They would therefore reduce the degree by which the speedometer is advanced if the tyres are not yet worn. The same applies where the positive tolerances given in the above table are used. In this instance it is also possible that even a very precise speedometer could display too low a speed.

2.2.10 Tyre profiles

The design of tyre profiles (Fig. 2.19) depends on the intended use, taking into account the parameters of height-to-width ratio, construction and mixture and design. The aquaplaning properties are improved by increasing the negative proportion (light places in the tyre impression, Fig. 2.9). The shoulder region with its transverse water-drainage grooves is particularly important for its properties in a lateral direction and the middle region with straight longitudinal grooves is important for its properties in a longitudinal direction. An asymmetrical profile design ('sports' profile) is chosen for wide tyres, tread lugs in the outside shoulder, which are subject to greater stress during cornering, can be designed to be more rigid. By adjusting the correct balance between profile rigidity and belt rigidity, it must be ensured that no conical forces are produced. Profiled bands around the middle region increase noise reduction and improve the steering response properties and, via the increase in circular rigidity, the brake response properties.

Winter tyre profiles are improved, in terms of their force transmission properties in the wet, snow and ice, by a higher negative profile component, transverse grooves and a large number of sipes. Directional profiles (TS770) can be used to increase water dispersal, the longitudinal force coefficient and self-cleaning by means of transverse grooves which run diagonally outwards. Noise control is improved by variation in block length, sipes cut up to under the groove base or ventilation grooves running around the tyre.

2.3 Wheels

2.3.1 Concepts

Tyres are differentiated according to the loads to be carried, the possible maximum speed of the vehicle, and whether a tubed or tubeless tyre is driven. In the case of a tubeless tyre, the air-tightness of the rim is extremely important. The wheel also plays a role as a 'styling element'. It must permit good brake ventilation and a secure connection to the hub flange (see Chapter 9, in Ref. [6]). Figure 2.20 shows a passenger car rim fitted with a tubeless tyre.

2.3.2 Rims for passenger cars, light commercial vehicles and trailers

For these types of vehicle only well-base rims are provided. The dimensions of the smallest size, at 12″ and 13″ diameter and rim width up to 5.0″, are contained in the standard DIN 7824. The designation for a standard rim, suitable for the 145 R 13 tyre (Fig. 2.1) for example is:

DIN 7824 – drop base rim 4.00 B × 13

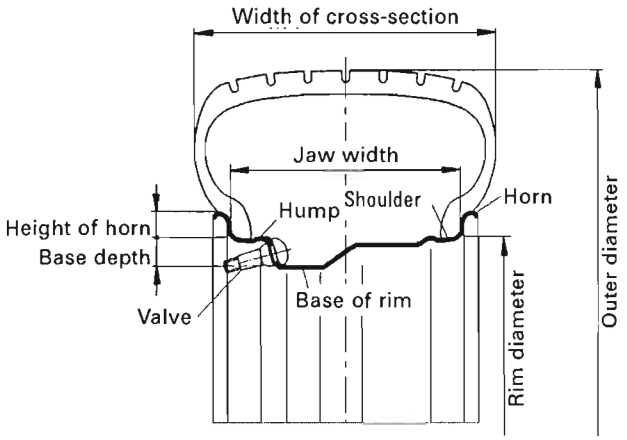

Fig. 2.20 Series 55 wide tyre designs, mounted on a double hump rim with the inflating valve shown in Fig. 2.6. The actual rim consists of the following:

- rim horns, which form the lateral seat for the tyre bead (the distance between the two rims is the jaw width a);
- rim shoulders, the seat of the beads, generally inclined at 5° ± 1° to the centre where the force transfer occurs around the circumference (Fig. 2.5);
- well base (also known as the inner base), designed as a drop rim to allow tyre fitting, and mostly shifted to the outside (diagram: Hayes Lemmerz).

This type of rim used on passenger cars up to around 66 kW (90 PS) has only a 14 mm high rim flange and is identified with the letter B. The DIN standard can generally be dropped.

In order to make it possible to fit bigger brakes (Fig. 2.10), more powerful vehicles have larger diameter rims as follows:

- series production passenger cars: 14″ to 17″ rims
- sports cars: 16″ to 18″ rims.

The J rim flange applied here is used on rims from 13″ upwards and is 17.3 mm high. The rim base can (as shown in Fig. 2.1) be arranged symmetrically or shifted outwards. The rim diameter, which is larger on the inside, creates more space for the brake (Figs 1.8, 1.56, 2.10, 2.11 and 2.20). DIN 7817 specifies the rim widths from 3½″ to 8½″. The definition of a normal asymmetrical rim with a 5″ width, J rim flange and 14″ diameter is:

DIN 7817 drop base rim – 5 J × 14

The symmetrical design is identified by the suffix 'S'. The standards also contain precise details on the design and position of the valve hole (see also Figs 2.20 and 2.24).

C tyres for light commercial vehicles require a broader shoulder (22 mm

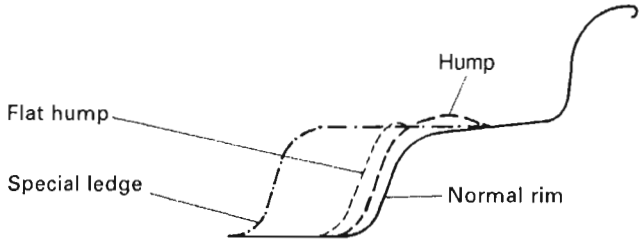

Fig. 2.21 Standard rim and contours of the safety shoulders which can be used on passenger cars and light commercial vehicles.

instead of 19.8 mm), which can be referred to by adding the letters LT (light truck) at the end of the marking:

DIN 7817 drop base rim – $5\frac{1}{2}$ J × 15 – LT

There is a preference worldwide for using tubeless radial tyres on passenger cars and light commercial vehicles. Where these tyres are used, it is essential to have a 'safety contour' at least on the outer rim shoulder. This stops air suddenly escaping if the vehicle is cornering at reduced tyre pressure.

The three different contours mainly used are (Fig. 2.21):

Hump	(H, previously H1)
Flat-hump	(FH, previously FHA)
Contre Pente	(CP)

Sheets 2 and 3 of DIN 7817 specify the dimensions of the first two designs. The 'hump' runs around the rim, which is rounded in H designs, whereas a flat hump rim is simply given a small radius towards the tyre foot. The fact that the bead sits firmly between the hump and rim flange is advantageous on both contours. An arrangement on both the outside and inside also prevents the tyre feet sliding into the drop bases in the event of all the air escaping from the tyre when travelling at low speeds, which could otherwise cause the vehicle to swerve. The disadvantage of hump rims is that changing the tyre is difficult and requires special tools.

A French design, intended only for passenger car rims, is the 'Contre Pente' rim, known as the CP for short. This has an inclined shoulder towards the rim base, which for rim widths between 4″ and 6″ is provided on one or both sides.

For years, the rims of most passenger cars have had safety shoulders on both sides, either a double hump (Figs 2.20 and 2.24) or the sharp-edged flat-hump on the outside and the rounder design on the inside (Fig. 2.23). The desired contour must be specified in the rim designation. Figure 2.22 gives the possible combinations and abbreviations which must appear after the rim diameter data. A complete designation for an asymmetrical rim would then be as follows:

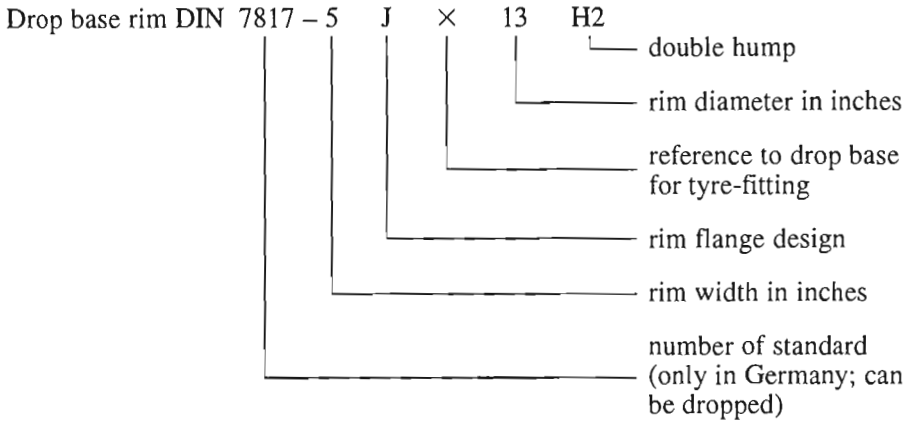

Fig. 2.22 Marking of the various safety shoulders when used only on the outside of the rim or on both the inside and outside. Normal means there is no safety contour (Fig. 2.1). Further details are contained in standard DIN 7817.

	Nature of safety shoulder		
Denomination	*Outside of rim*	*Inside of rim*	*Identification letters*
One-sided hump	Hump	Normal	H
Double hump	Hump	Hump	H2
One-sided flat hump	Flat hump	Normal	FH[1]
Double-sided flat hump	Flat hump	Flat hump	FH2[1]
Combination hump	Flat hump	Hump	CH[2]

[1] In place of the identification letters FH the identification letters FHA were also permitted.
[2] In place of the identification letters CH the identification letters FH1-H were also permitted.

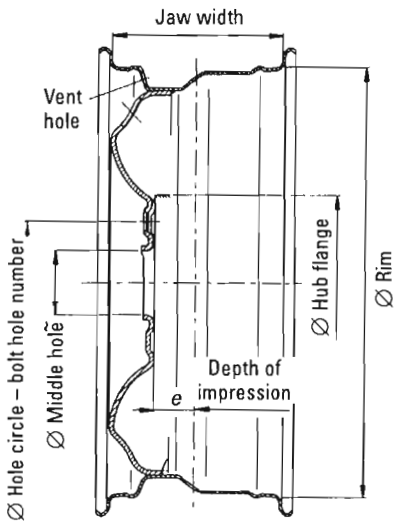

Fig. 2.23 The sheet metal disc-type wheel used in series production vehicles consists of a rim and disc. To avoid fatigue fractures, the wheel hub flange diameter should be greater than the dish contact surface. Wheel offset e (depth of impression) and kingpin offset at ground r_σ are directly correlated. A change in e can lead to an increase or a reduction in r_σ.

The dome-shaped dish leading to the negative kingpin offset at ground is clearly shown (diagram: Hayes Lemmerz).

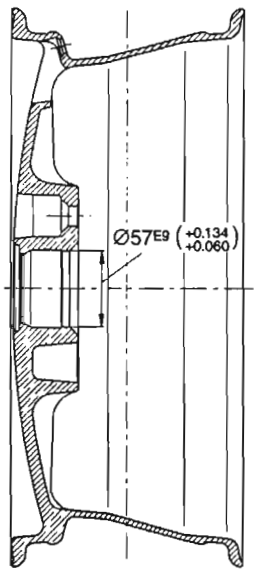

Fig. 2.24 Hayes Lemmerz alloy wheel for the Audi 80, made of the aluminium alloy GK-Al Si 7 Mg wa. The wheel has a double-hump rim (H2) and middle centring and is fixed with four spherical collar bolts. The different wall thicknesses, which are important for the strength, the shape of the bolt hole, the different shape of the drop-rim and the position of the valve hole are clearly shown. At high speeds the snap-fit valve (Fig. 2.6) is pressed outwards by the centrifugal force and supported below the rim base.

2.3.3 Wheels for passenger cars, light commercial vehicles and trailers

Most passenger cars and light commercial vehicles are fitted with sheet metal disc wheels, because these are economic, have high stress limits and can be readily serviced. They consist of a rim and a welded-on wheel disc (also known as an attachment face, Fig. 2.23). Cold-formable sheet metal, or band steel with a high elongation, can be used (e.g. RSt37-2 to European standard 20) depending on the wheel load, in thicknesses from 1.8 to 4.0 mm for the rim and 3.0 to 6.5 mm for the attachment faces.

There is a direct correlation between wheel offset e and 'kingpin offset at ground' r_σ; the more positive r_σ, the smaller can be the depth dimension e. However, a negative kingpin offset $-r_\sigma$, especially on front-wheel drive, results in a significant depth e and severe bowing of the attachment faces (as can be seen in Figs 2.8, 2.23, 2.25 and 3.102 and Section 7.3 in Ref. [6]).

The wheel disc can be perforated to save weight and achieve better brake cooling. Despite the fact that they cost almost four times as much as sheet metal designs, alloy wheels are becoming increasingly popular (Figs 1.56 and 2.24). Their advantages are:

- lower masses;
- extensive styling options; and therefore
- better appearance;
- processing allows precise centring and limitation of the radial and lateral runout (see Section 2.5);
- good heat transfer for brake-cooling (see Chapter 9 in Ref. [6]).

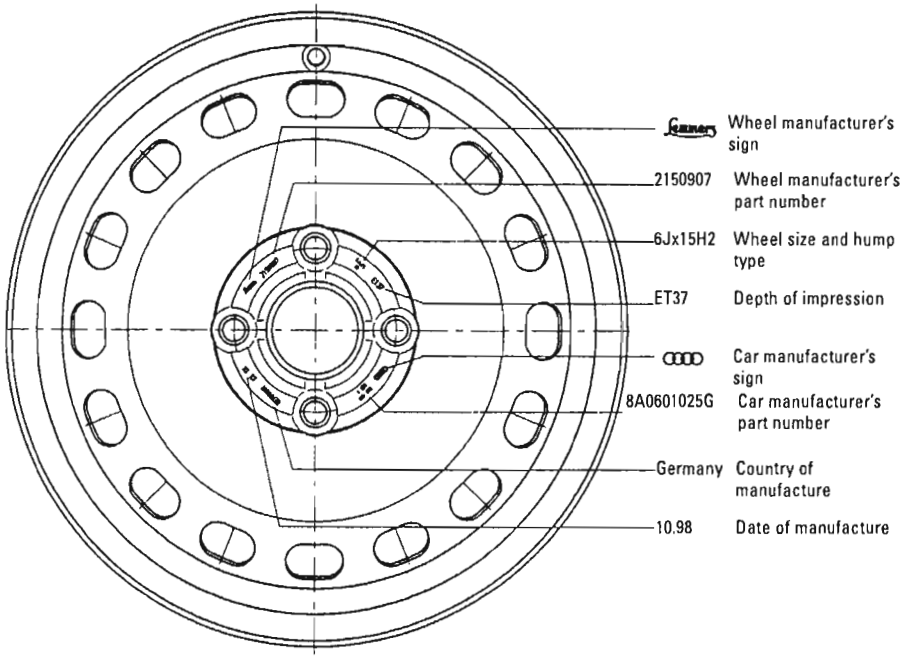

Fig. 2.25 Double-hump sheet metal disc-type wheel with openings for cooling the brakes. Also pictured is the stamp in accordance with the German standard DIN 7829, indicating manufacturer code, rim type and date of manufacture (week or month and year).

Also specified is the wheel offset (ET37) and, in the case of special wheels with their own ABE (General operating approval), the allocation number of the KBA, the German Federal Vehicle Licensing Office. If there is not much space the stamp may be found on the inside of the dish. The date of manufacture also points to when the vehicle was manufactured (diagram: Hayes Lemmerz).

Often incorrectly called aluminium rims, alloy wheels are mainly manufactured using low-pressure chill casting, occasionally forging or aluminium plate, and generally consist of aluminium alloys with a silicon content (which are sometimes heat hardenable), such as GK-Al Si 11 Mg, GK-Al Si 7 Mg T (T = tempered after casting) etc.

Regardless of the material, the wheels must be stamped with a marking containing the most important data (Fig. 2.25).

2.3.4 Wheel mountings

Many strength requirements are placed on the wheel disc sitting in the rim (or the wheel spider on alloy wheels); it has to absorb vertical, lateral and longitudinal forces coming from the road and transfer them to the wheel hub via the fixing bolts.

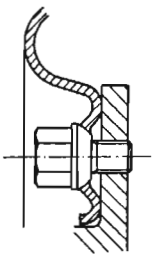

Fig. 2.26 Depression design with special springing characteristics on a passenger car sheet metal disc-type wheel. The wheel can be centred using the fixing bolts or by fitting into the toleranced hole (Fig. 2.24).

The important thing here is that the contact area of the attachment faces, known as the 'mirror', should sit evenly and, for passenger cars, that the hub flange should have a slightly larger diameter (Fig. 2.23), otherwise it is possible that the outer edge of the hub will dig into the contact area, with a loss of torque on the bolts. The notch effect can also cause a fatigue fracture leading to an accident.

The number of holes and their circle diameter are important in this context. This should be as large as possible to introduce less force into the flange and fixing bolts. If the brake discs are placed onto the wheel hub from the outside – which is easier from a fitting point of view – it is difficult to create a hole larger than 100 mm on 13″ wheels, and using a 14″ or 15″ wheel should make for the best compromise (Figs 1.8, 1.41, 1.44 and 2.10). German standard DIN 74361 contains further details.

The brake disc can also be fixed to the wheel hub from the inside (Fig. 1.38). However, the disadvantage of this is that the hub has to be removed before the disc can be changed. This is easy on the non-driven axle, but time-consuming on the driven axle (see Section 2.5 in Ref. 2 and Chapter 9 in Ref. 6). This brief look shows that even the brakes play a role in the problems of fixing wheels.

Nowadays, wheels are almost always fixed with four or five metric M12 × 1.5 or M14 × 1.5 DIN 74361 spherical collar bolts. The high friction between the spherical collar and the stud hole prevents the bolts from coming loose while the vehicle is in motion. For this reason, some car manufacturers keep the contact surface free of paint. On sheet metal disc wheels with attachment faces up to 6.5 mm thick, the spring action of the hole surround (Fig. 2.26) is an additional safety feature, which also reduces the stress on the wheel bolts as a result of its design elasticity. Sheet metal rings are often inserted in the alloy wheels to withstand high stresses underneath the bolt head.

Generally, the spherical collar nuts also do the job of centring the wheels on the hub. Hub centring has become increasingly popular because of a possible hub or radial run-out and the associated steering vibrations. A toleranced collar placed on the hub fits into the dimensioned hole which can be seen in Fig. 2.24.

2.4 Springing behaviour

The static tyre spring rate c_T – frequently also known as spring stiffness or (in the case of a linear curve) spring constant – is the quotient of the change in vertical

force $\Delta F_{Z,W}$ in Newtons and the resultant change Δs_T – the compression in mm within a load capacity range corresponding to the tyre pressure p_T (Fig. 2.27; see also Section 2.2.5.4):

$$c_T = \Delta F_{Z,W}/\Delta s_T \ (\mathrm{N/mm^{-1}}) \tag{2.3}$$

The parameter c_T forms part of the vibration and damping calculation and has a critical influence on the wheel load impact factor (see Section 5.2 in Ref. [3], Section 4.1). The stiffer the tyre, the higher the damping must be set and the greater the stress experienced by the chassis components. The following parameters influence the spring rate:

- vertical force
- tyre pressure
- driving speed
- slip angle
- camber angle
- rim width

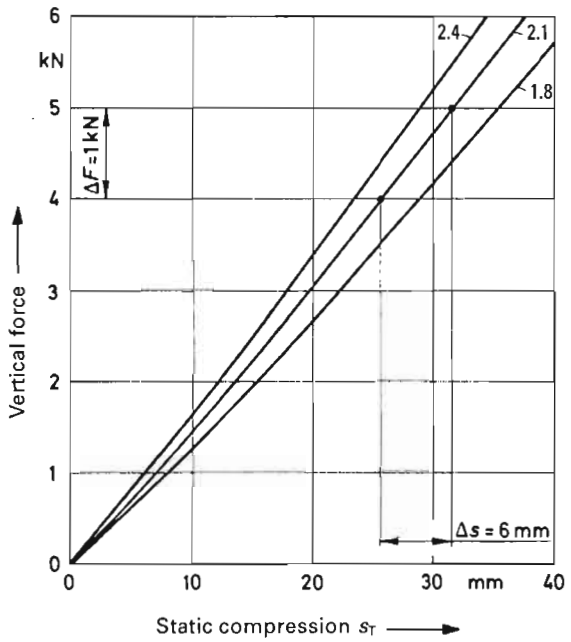

Fig. 2.27 The static tyre spring rate c_T is the quotient of the force and the deflection travel shown on the radial tyre 175/70 R 13 80 S at p_T = 1.8 bar, 2.1 bar and 2.4 bar; the example shown gives:

$$C_T = \frac{\Delta F_{Z,W}}{\Delta S_T} = \frac{1000\ \mathrm{N}}{6\ \mathrm{mm}} = 167\ \mathrm{N/mm}$$

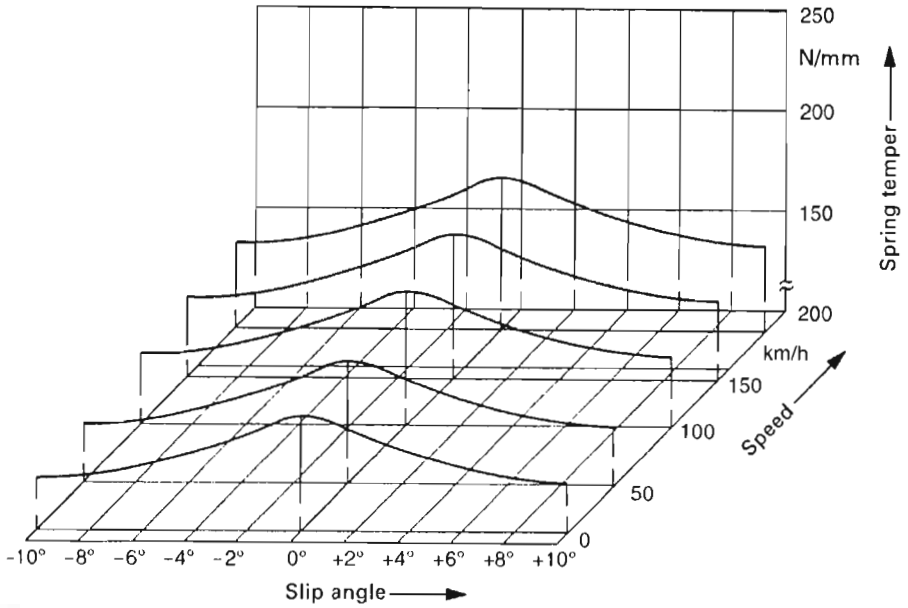

Fig. 2.28 Tyre springing rate as a function of slip angle and road speed, measured on a radial tyre 185/70 R 13 86 S at p_T = 2.1 bar. Speed increases the springing rate as the belt stands up due to the centrifugal force. However, the slip angle makes it softer because the belt is pushed away to the side and the shoulders take over part of the springing effect.

- height-to-width ratio
- construction of tyre (bias angle, material)
- tyre wear and tear
- wheel load frequency.

As can be seen in Fig. 2.27, apart from in the low load range, the spring rate is independent of the load. A linear increase can be seen as the speed increases (Figs 2.16 and 2.28; see also Equation 5.5a), which persists even when the tyre pressure changes.

During cornering, the force F_{YW} (Fig. 3.119) shifts the belt in a lateral direction, and so it tips relative to the wheel plane. This leads to a highly asymmetrical distribution of pressure and (as can be seen from Fig. 2.28) to a reduction in the spring rate as the slip angles increase.

2.5 Non-uniformity

The tyre consists of a number of individual parts, e.g. carcass layers, belt layers, running tread, sidewall stock and inner lining, which – put together on a tyre

rolling machine – give the tyre blank (Fig. 2.5). In the area where it is put together, variations in thickness and stiffness occur, which can lead to non-uniformity.

Owing to the irregularities caused during manufacture, the following occur around the circumference and width of the tyre:

- thickness variations
- mass variations
- stiffness variations.

These cause various effects when the tyre rolls:

- imbalance
- radial tyre runout
- lateral tyre runout
- variation in vertical and/or radial force
- lateral force variations
- longitudinal force variation
- ply steer (angle) force
- conicity force.

Imbalance U occurs when an uneven distribution of mass and the resulting centrifugal forces are not equalized. Because the uneven distribution occurs not only around the circumference, but also laterally, we have to differentiate between static and dynamic imbalance (Fig. 2.29). This is calculated in size and direction on balancing machines and eliminated with balancing weights on the rim bead outside and inside the wheel.

Radial and lateral runout are the geometrical variations in the running tread and the sidewalls. They are measured with distance sensors on a tyre-uniformity machine. The German WdK Guideline 109 contains full details.

The most important of the three force variations is the radial force variation. For greater clarity, it is shown on the model in Fig. 2.30, where the tyre consists of different springs whose rates fluctuate between c_1 and c_8. The resulting phenom-

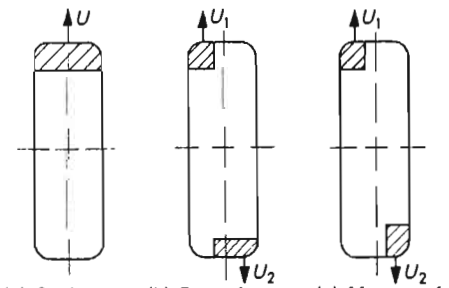

Fig. 2.29 Different forms of imbalance U: (a) static, (b) dynamic. The imbalance is equalized in (c).

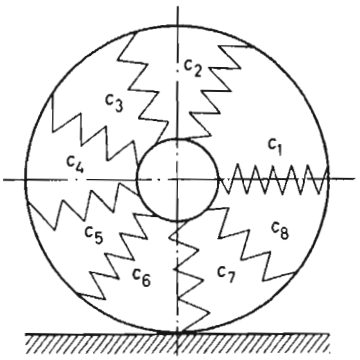

Fig. 2.30 The tyre spring rate can fluctuate depending on the manufacturing process, shown as c_1 to c_8.

ena should be indicated on the 175 R 14 88 S steel radial tyre, loaded at $F_{Z,W}$ = 4.5 kN and pressurized to p_T = 1.9 bar. Assuming this had a mean spring rate c_T = 186 N m^{-1}, which fluctuates by ±5%, the upper limit would be $c_{T,max}$ = 195 N mm^{-1} and the lower limit would be $c_{T,min}$ = 177 N mm^{-1}. Under vertical force $F_{Z,W}$ = 4.5 kN = 4500 N the tyre would, according to Equation 2.3a, have as its smallest jounce travel

$$s_{T,min} = \frac{F_{Z,W}}{C_{T,max}} = \frac{4500}{195}; \qquad s_{T,min} = 23.1 \text{ mm} \tag{2.3a}$$

and

$$s_{T,max} = 25.4 \text{ mm}$$

as the greatest travel. The difference is

$$\Delta s_T = s_{T,max} - s_{T,min} = 2.3 \text{ mm}$$

This difference in the dynamic rolling radius of Δs_T = 2.3 mm would cause variations in vertical force $\Delta F_{Z,W}$, which nevertheless is still smaller than the friction in the wheel suspension bearings. At a speed of perhaps 120 km/h and travelling on a completely smooth road surface, this would nevertheless lead to vibration that would be particularly noticeable on the front axle.

The vehicle used as an example should have a body spring rate of c_f = 15 N/mm per front axle side. The travel Δs_T would then give a vertical force difference, in accordance with Equation 5.0a, of:

$$\Delta F_{Z,W,f} = c_f \Delta s_T = 15 \times 2.3; \qquad \Delta F_{Z,W,f} = 34.5 \text{ N}$$

The friction per front axle side is, however, not generally below

$$F_{fr} = \pm 100 \text{ N (Fig. 5.6)}$$

so it can only be overcome if greater variations in vertical force occur as a result of non-uniformity in the road surface. The more softly sprung the vehicle, the more the variations in radial force in the tyre make themselves felt (see Section 5.1.2).

The lateral force variations of the tyre influence the straight-running ability of the vehicle. Even with a tyre that is running straight, i.e. where the slip angle is zero, lateral forces occur, which also depend on the direction of travel (see Chapter 11 in Ref. [4]).

The variations in longitudinal force that occur must be absorbed on the chassis side by the rubber bearings described in Section 3.6.5.2.

The ply steer force dependent on the rolling angle results from the belt design because of the lateral drift of the tyre contact area as a consequence of flat spotting. In contrast, the conicity force, resulting from a change in diameter across the width of the tyre, is not dependent on the rolling angle. Both forces disturb the straight running of the vehicle (see Chapter 11 in Ref. [4]).

2.6 Rolling resistance

2.6.1 Rolling resistance in straight-line driving

Rolling resistance is a result of energy loss in the tyre, which can be traced back to the deformation of the area of tyre contact and the damping properties of the rubber. These lead to the transformation of mechanical into thermal energy, contributing to warming of the tyre.

Sixty to 70% of the rolling resistance is generated in the running tread (Fig. 2.5) and its level is mainly dependent on the rubber mixture. Low damping running tread mixtures improve the rolling resistance, but at the same time reduce the coefficient of friction on a wet road surface. It can be said that the ratio is approximately 1:1, which means a 10% reduction in the rolling resistance leads to a 10% longer braking distance on a wet road surface. The use of new combinations of materials in the running tread (use of silica) has led to partial reduction of the conflict between these aims.

Rolling resistance is either expressed as a rolling resistance force F_R or as the rolling resistance factor k_R – also known as the coefficient of rolling resistance:

$$F_R = k_R \times F_{Z,W} \text{ (N)} \tag{2.4}$$

The factor k_R is important for calculating the driving performance diagram and depends on the vertical force $F_{Z,W}$ and the tyre pressure p_T. Figure 2.31 shows the theoretical k_R curve of tyres of different speed classes as a function of the speed. Although the coefficient of rolling friction of the T tyre increases disproportionally from around 120 km h^{-1}, this increase does not occur in H and V tyres until 160 to 170 km h^{-1}. The reason for this behaviour is the shape of the rolling hump that occurs at different speeds depending on the speed class, and is dependent on the stiffness of the belt, in other words on its design. The lower k_R values for the T tyres result from the usually poorer wet skidding behaviour of this speed class.

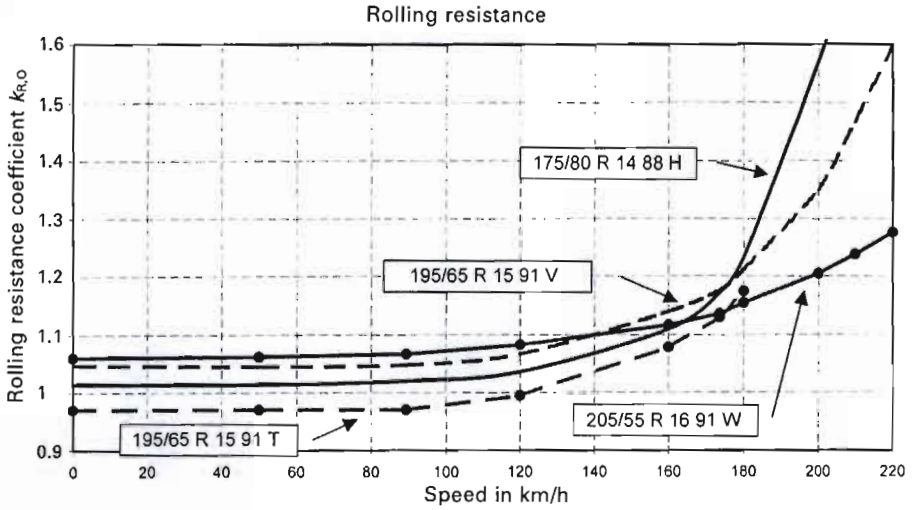

Fig. 2.31 Rolling resistance coefficients $k_{R,0}$, average values of radial tyres as a function of the speed, measured on a drum test rig. Tyres authorized up to 210 km h^{-1} have a lower rolling resistance below 160 km h^{-1} (than the V and W designs) whilst the value rises sharply above this speed (measurements: Continental).

Asphalted roads cause $k_{R,0}$ to increase by around 20% as k_R and rough concrete to at least 30%. The ratios i_R are then 1.2 or 1.3 to 1.4 and the actual value of k_R is:

$$k_R = i_R \times k_{R,0} \qquad (2.4a)$$

The difference is due to the different design emphases during development of the tyres. The design priorities for H, V and W tyres are high-speed road holding and good wet skidding and aquaplaning behaviour, whereas T tyres are designed more for economy, i.e. lower rolling resistance (which plays an important role at lower speeds and influences urban driving fuel consumption, Fig. 2.32) and long service life.

2.6.2 Rolling resistance during cornering

Rolling resistance can change dramatically during cornering; its value depends on the speed and the rolling radius R, in other words on $\mu_{Y,W}$ (see Equations 2.9 and 2.11 and Fig. 2.43) and $\alpha_{f\,or\,r}$. The rolling resistance $k_{R,co}$, which is included in some calculations (see Equation 3.35), comprises the coefficient k_R for straight running and the increase Δk_R:

$$k_{R,co} = k_R + \Delta k_R$$

$$\Delta k_R \approx \mu_{Y,W} \times \sin \alpha \qquad (2.4b)$$

The following data can provide an example:

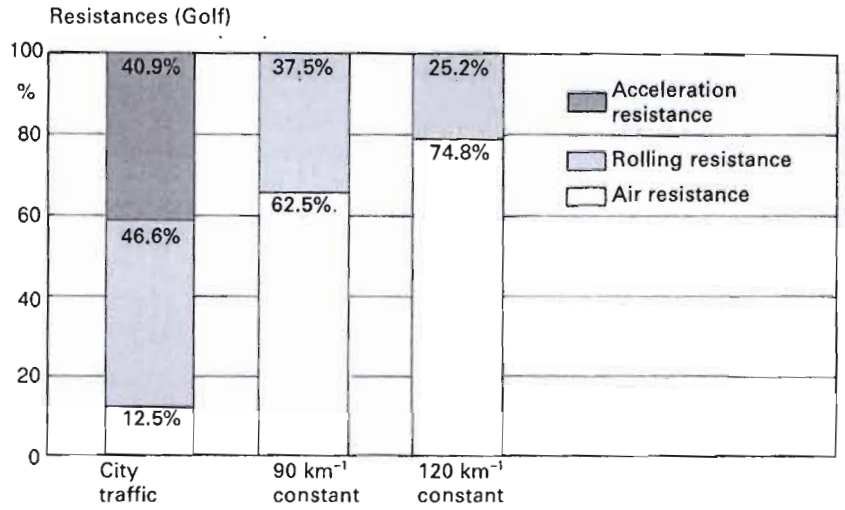

Fig. 2.32 In town and when the vehicle is travelling at low speeds on rural roads, fuel consumption is determined up to 40% by the rolling resistance, whereas at higher speeds the air drag is the determining factor see Section 2.1 and Section 2.2 in Ref. [3]). The figure shows a study carried out by VW on the Golf.

Front axle force $F_{Z,V,f} = 7\text{kN}$; $\mu_{Y,W} = 0.7$ (asphalted road)
Tyres 155 R 13 78 S $p_T = 1.8$ bar, $v \leqslant 120$ km h

In accordance with Equation 2.11 related to one wheel:

$$F_{Y,W,f} = \mu_{Y,W} F_{Z,W,f} = \mu_{Y,W} F_{Z,V,f}/2 = 0.7 \times 3.5 \text{ kN}$$
$$F_{Y,W,f} = 2.45 \text{ kN}$$

The slip angle read off at $F_{Y,W,f}$ in Fig. 2.44 is 4° and corresponds to the values in Fig. 2.43.

However, the dynamic wheel load transfer seen in Fig. 1.5 plays a role during cornering, leading to a greater slip angle on the wheel on the outside of the curve (and thus also on the inner wheel), than resulted from test rig measurements. On '82' series tyres, α is about 5°, in accordance with Fig. 2.38:

$$\alpha \approx 7\, \mu_{Y,W} \qquad (2.4c)$$

With sin 5° in accordance with Equation 2.4b there is an increase of

$$\Delta k_R \approx 0.7 \times 0.087 = 0.061$$

Assuming a value of $k_{R,0} = 0.012$, in accordance with Equation 2.4a, on asphalted road

$$k_R = i_R \, k_{R,0} = 1.2 \times 0.010 = 0.012$$

and therefore the rolling resistance during cornering is

$$k_{R,co} = 0.012 + 0.061 \approx 0.073$$

In the case of the understeering vehicles (Fig. 2.41) $k_{R,co}$ increases as a result of the additional steering input and – if the wheels are driven – μ_{rsl} should be inserted for $\mu_{Y,W}$ (see Equation 2.18); the slip angle increases further. '65 Series' tyres, on the other hand, require a smaller steering input and thus make the vehicle easier to handle:

$$\alpha = 3 \times \mu_{Y,W} \tag{2.4d}$$

2.6.3 Other influencing variables

The rolling resistance increases in certain situations:

- in the case of a large negative or positive camber (the influence can be ignored up to $\pm 2°$);
- due to a change to track width (Fig. 3.6);
- in the case of deviations in zero toe-in around 1% per $\delta = 10'$ or $v = 1$ mm;
- on uneven ground.

In general it can be said that the ratio i_R (see Fig. 2.31) will take the following values:

- around 1.5 on cobbles
- around 3 on potholed roads
- around 4 on compacted sand
- up to 20 on loose sand.

2.7 Rolling force coefficients and sliding friction

2.7.1 Slip

If a tyre transfers drive or braking forces, a relative movement occurs between the road and tyre, i.e. the rolling speed of the wheel is greater or less than the vehicle speed (see Equation 2.1b). The ratio of the two speeds goes almost to ∞ when the wheel is spinning, and is 0 when it locks. Slip is usually given as a percentage. The following equation applies during braking:

$$S_{X,W,b} = \frac{\text{vehicle speed} - \text{circumferential speed of wheel}}{\text{vehicle speed}}$$

$$S_{X,W,b} = \frac{v - v_W}{v} \times 100\ (\%) \tag{2.4e}$$

Drive slip is governed by:

$$S_{X,W,a} = \frac{v_W - v}{v_W} \times 100\ (\%) \tag{2.4f}$$

The different expressions have the advantage that, in both cases where the wheel is spinning or locked, the value is 100% and is positive.

Further details can be found in Section 2.2.8, in Ref. 6 (Section 1.2), Ref. 7 (Chapter 1) and in Ref. 9 (Section 2.2).

2.7.2 Friction coefficients and factors

The higher the braking force or traction to be transmitted, the greater the slip becomes. Depending on the road condition, the transferable longitudinal force reaches its highest value between 10% and 30% slip and then reduces until the wheel locks (100% slip). The quotient from longitudinal force F_x and vertical force $F_{Z,W}$ is the coefficient of friction, also known as the circumferential force coefficient

$$\mu_{X,W} = F_{X,W}/F_{Z,W} \tag{2.5}$$

when it relates to the maximum value, and the coefficient of sliding friction, also called sliding friction factor

$$\mu_{X,W,lo} = F_{X,W}/F_{Z,W} \tag{2.5a}$$

when it is the minimal value (100% slip) (Fig. 2.33). F_x is designated $F_{X,W,b}$ during braking and $F_{X,W,a}$ during traction.

In all cases $\mu_{X,W}$ is greater than $\mu_{X,W,lo}$; in general it can be said that

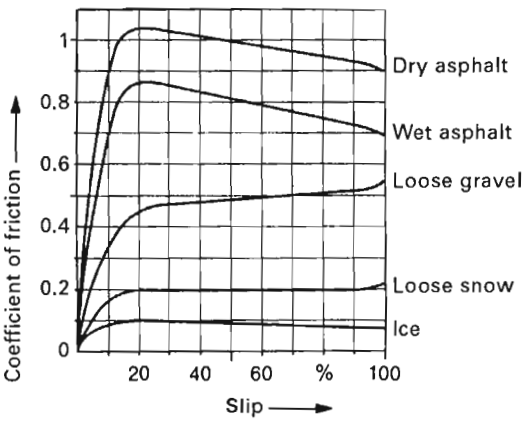

Fig. 2.33 Coefficient of friction $\mu_{X,W}$ of a summer tyre with 80 to 90% deep profile, measured at around 60 km/h and shown in relation to the slip on road surfaces in different conditions (see also Fig. 1.64). Wide tyres in the '65 series' and below have the greatest friction at around 10% slip, which is important for the ABS function (see Chapter 1 in Ref. [7]).

on a dry road $\mu_{X,W} \approx 1.2\ \mu_{X,W,lo}$ (2.6)

on a wet road $\mu_{X,W} \approx 1.3\ \mu_{X,W,lo}$ (2.6a)

2.7.3 Road influences

2.7.3.1 Dry and wet roads

On a dry road, the coefficient of friction is relatively independent of the speed (Fig. 2.34), but a slight increase can be determined below 20 km/h. The reason lies in the transition from dynamic to static rolling radius (see the example in Section 2.2.5.4) and is therefore linked to an increasing area of tyre contact. At speeds a little over zero, on a rough surface, a toothing cogging effect can occur, which causes a further increase in the coefficient of friction, then:

$$\mu_{X,W} \geqslant 1.3 \tag{2.6b}$$

When the road is wet, the coefficient of friction reduces, but is still independent of the speed. This situation changes as the amount of water increases and also with shallower profile depth. The water can no longer be moved out of the profile grooves and the μ value falls as speed increases.

2.7.3.2 Aquaplaning

The higher the water level, the greater the risk of aquaplaning. Three principal factors influence when this occurs:

- road
- tyres
- speed.

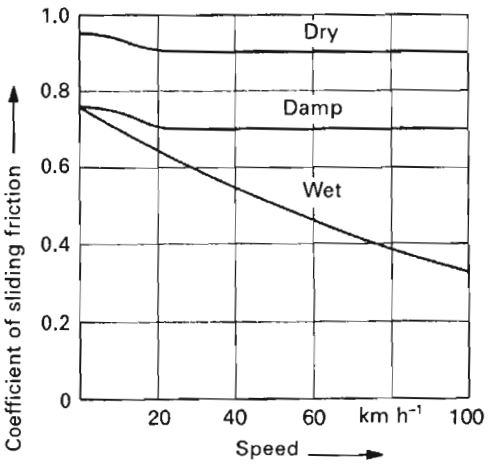

Fig. 2.34 Dependency of the coefficient of sliding friction $\mu_{X,W,lo}$ on speed on different road conditions.

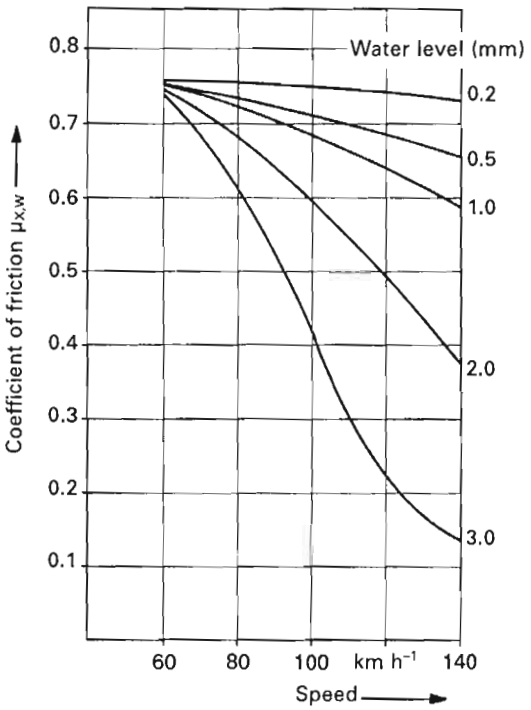

Fig. 2.35 Coefficients of friction $\mu_{x,w}$ of a summer tyre with an 8 mm deep profile dependent on speed at different water levels. Hardly any influence can be detected under 60 km h^{-1}; at higher speeds and 3 mm water depth, the curve shows a lowering of $\mu_{x,w}$ which indicates the aquaplaning effect.

With regard to the road, the water level is the critical factor (Fig. 2.35). As the level rises, there is a disproportionate increase in the tendency towards aquaplaning. When the level is low, the road surface continues to play a role because the coarseness of the surface absorbs a large part of the volume of water and carries it to the edge of the road. Following rainfall, the water levels on roads are generally up to 2 mm; greater depths can also be found where it has been raining for a long time, during storms or in puddles.

On the tyre, the tread depth has the greatest influence (Fig. 2.47). There can be up to a 25 km h^{-1} difference in speed between a full tread and the legal minimum tread depth of 1.4 mm. High tyre pressure and low running surface radius r (Fig. 2.5) lead to the area of contact becoming narrower, giving the advantage of improved aquaplaning behaviour as the distribution of ground pressure becomes more even (Fig. 2.9). Lower tyre pressure and contours with larger radii make aquaplaning more likely; this also applies to wider tyres (Fig. 2.19) particularly when tread depths are low. However, the greatest influence by far is the speed, especially when the water level increases and tread depths are low. This is why reducing speed is the best way to lessen the risk of aquaplaning, and is a decision drivers can make for themselves.

2.7.3.3 Snow and ice

Similar to aquaplaning, low coefficients of friction occur on icy roads, although these are highly dependent on the temperature of the ice. At close to 0°C, special

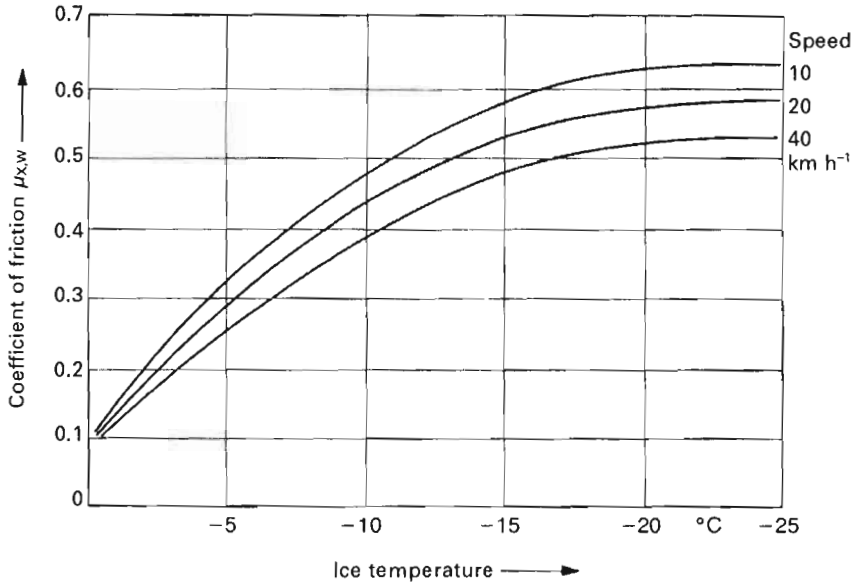

Fig. 2.36 Influence of ice temperature and car speed on the coefficient of friction $\mu_{x,w}$ of an 82 series winter tyre; the extremely low values at 0°C can be seen clearly.

conditions occur; compression of the surface can lead to the formation of water which has a lubricating effect and reduces the coefficient of friction to $\mu_{x,w} \leqslant 0.08$ (Fig. 2.36). At −25°C, a temperature that is by no means rare in the Nordic countries, values of around $\mu_{x,w} = 0.6$ can be reached. At low temperatures, coefficients of friction and sliding friction are further apart:

$$\mu_{x,w} \sim 2\,\mu_{x,w,lo} \tag{2.7}$$

2.8 Lateral force and friction coefficients

2.8.1 Lateral forces, slip angle and coefficient of friction

Lateral forces on a rolling tyre can be caused by the tyre rolling diagonal to the direction of travel (so-called slip), the tendency of a tyre to move from its position vertical to the road, camber or conical effects. The build-up of lateral forces as a result of slip will be discussed next.

If a disturbing force $F_{c,y}$ acts at the centre of gravity of the vehicle (e.g. a wind or side negative lift force), lateral wheel forces $F_{y,w,f,o}$, $F_{y,w,f,i}$, $F_{y,w,r,o}$ and $F_{y,w,r,i}$ are needed to balance the forces (Fig. 2.37). To build up these forces, the vehicle must alter its direction of travel about the angle α, the slip angle. The size of the slip angle depends on the force transmission properties of the tyre and the disturbing force (Fig. 2.38).

When cornering, the interference force should be equal to the centrifugal force $F_{c,V}$, which results from the speed v in m/s and the radius of the bend R in m, on which the vehicle centre of gravity V (Fig. 2.29a) moves. With the total weight $m_{V,t}$ of the vehicle the equation is:

$$F_{c,V} = m_{V,t} \times v^2/R = m_{V,t} \times a_y = F_{Y,V} \text{ (N)} \tag{2.8}$$

The centrifugal or disturbance force is just as large as the lateral forces on the wheels (Fig. 2.37):

$$F_{Y,V} = F_{Y,W,f,o} + F_{Y,W,f,i} + F_{Y,W,r,o} + F_{Y,W,r,i} = \Sigma F_{Y,W} \tag{2.8a}$$

and

$$\Sigma F_{Y,W} = \mu_{Y,W} \times \Sigma F_{Z,W} = \mu_{Y,W} \times F_{Z,V,t}$$

Together the two equations give

$$\mu_{Y,W} F_{Z,V,t} = \mu_{Y,W} \times m_{V,t}\, g = m_{V,t} \times a_y \tag{2.9}$$

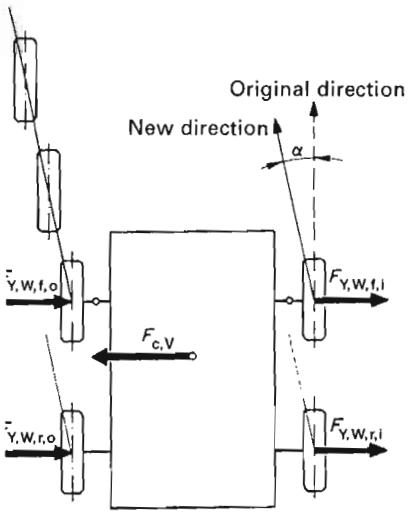

Fig. 2.37 Tyres are only able to transfer a lateral force $F_{Y,V}$ acting on the vehicle if they are rolling at an angle to the vehicle. Regardless of whether these are $F_{Y,V}$ or the centrifugal force $F_{C,Y}$ during cornering, the lateral forces $F_{Y,W}$ should be regarded as being perpendicular to the wheel centre plane.

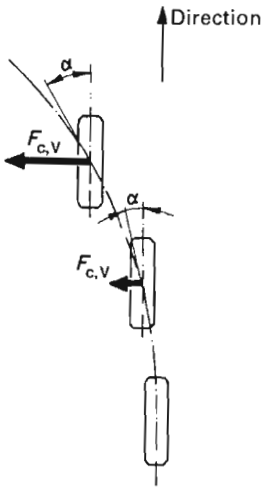

Fig. 2.38 The higher the lateral force $F_{Y,W}$, the greater the tyre slip angle α.

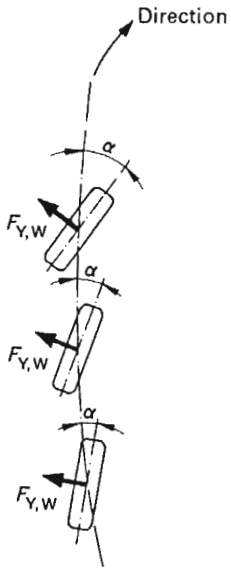

Fig. 2.39 Increasing lateral forces $F_{Y,W}$ during cornering caused by the centrifugal force $F_{c,V}$ leads to increasing slip angles α.

and

$$\mu_{Y,W} = g/a_y$$

The coefficient of friction $\mu_{Y,W}$ is not dependent on the radius of the curve and driving speed and is therefore more suitable for calculating cornering behaviour (see also Equation 6.13a).

The faster the vehicle negotiates a bend, the higher the coefficient of friction used and the greater the slip angles (Fig. 2.39).

2.8.2 Self-steering properties of vehicles

The self-steering properties of a vehicle describe the lateral force and hence slip angle ratios produced during steady-state cornering (radius and driving speed constant; no external disturbances). In the case of an understeering vehicle, a larger slip angle is required on the front axle than at the rear axle ($\alpha_f > \alpha_r$, Fig. 2.41). During cornering with an increase in lateral acceleration, the driver must force the vehicle into the bend by increasing the steering angle (see Fig. 5.2). If the necessary slip angles on the front and rear axles are the same ($\alpha_f = \alpha_r$, Fig. 2.40), one speaks of neutral handling characteristics. Over-steering behaviour is present if the tail of the vehicle moves outwards during cornering and the slip angle on the rear axle is greater than on the front axle ($\alpha_f < \alpha_r$, Fig. 2.42). The driver must respond to this by reducing the steering angle.

As understeering behaviour is consistent with the expectations and experience of the driver, it is this which needs to be aimed for. In normal driving conditions

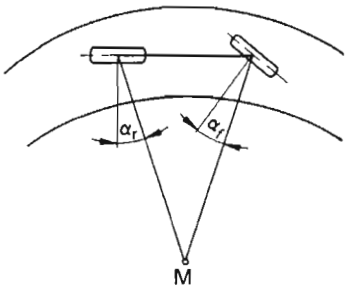

Fig. 2.40 If, during cornering, $\alpha_f \sim \alpha_r$, the handling of a vehicle can be described as neutral.

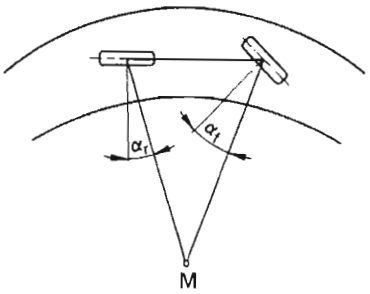

Fig. 2.41 If there is a greater slip angle α_f on the front wheels than α_r on the rear, the vehicle understeers.

Fig. 2.42 If there is a greater slip angle α_r on the rear wheels than on the front (α_f), the vehicle oversteers. The positive angle describes the angle between the vehicle longitudinal axis and its speed at the centre of gravity.

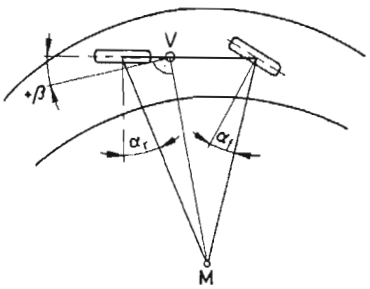

(anti-skid roadway, lateral acceleration of less than 6 m/s), all vehicles, therefore, are now designed to understeer. With increasing lateral acceleration, the understeering behaviour should be as linear as possible and then, also as a warning to the driver that the stability limit is about to be reached, increase progressively. If the handling characteristics change to oversteer at the stability limit, for instance with very high acceleration, this is an unpredictable driving situation which the untrained driver can only control with difficulty. For active riding safety, the predictability of self-steering properties in all kinds of conditions (vehicle loading, the distribution of driving torque in four-wheel drive vehicles, different coefficients of friction, acceleration or braking procedures, changes in tyre pressure, etc.) is of paramount importance.

For a simplified representation of the relationships described, the so-called single-track model is used, in which the wheels of the vehicle are drawn together in the middle of the vehicle, without taking into account the height of the centre of gravity (flat model).

Since in greater bend radii the average steering angle δ_m is less than 5°, it can be assumed that the sine and radius values of the angle are equal, and the angles δ_o and δ_i correspond to this (Fig. 3.91 and Equation 3.17):

$$\sin \delta_m \approx \delta_m \approx \delta_o \approx \delta_i \text{ (rad)}$$

Using Equation 3.12 it is now possible to determine the relationship between steering angle, turning circle diameter D_S (Figs 1.69 and 3.89) and slip angles at a constant cornering speed:

$$\delta_m = \frac{2 \times l}{D_S} + \alpha_f - \alpha_r \tag{2.10}$$

The kingpin offset at ground r_σ is so negligable in comparison to D_S that it can be ignored.

2.8.3 Coefficients of friction and slip

To determine the cornering behaviour, the chassis engineer needs the lateral forces (or the coefficient of friction) based on the slip angle and the parameters:

- vertical force (or wheel load) in the centre of tyre contact
- tyre pressure
- wheel camber
- tyre type.

The measurements are generally taken on test rigs, up to slip angles of $\alpha = 10°$. The drum surface with its friction values of $\mu_0 = 0.8–0.9$ sets limits here, and larger angles hardly give increasing lateral coefficients of friction:

$$\mu_{Y,W} = F_{Y,W}/F_{Z,W} \tag{2.11}$$

Conditions on the road are very different from those on the test rig; the type of road surface and its condition play a role here. As can be seen in Fig. 2.43, the coefficient of friction on rough, dry concrete increases to $\alpha = 20°$ and then falls. In precisely the same way as with the longitudinal force the slip $S_{Y,W}$ (in the lateral direction) is also taken into consideration; this is as a percentage of the sine of the slip angle times 100:

$$S_{Y,W} = \sin \alpha \times 100\ (\%) \tag{2.12}$$

In conjunction with the drum value $\alpha = 10°$, this would give a slip of $S_{Y,W} = 17\%$, and on the street at $\alpha = 20°$ slip values of up to $S_{Y,W} = 34\%$. If the tyre is further twisted to $\alpha = 90°$, it slides at an angle of 90° to the direction of travel; sin α would then be equal to one and $S_{Y,W} = 100\%$. The coefficient of friction then becomes the coefficient of lateral sliding friction $\mu_{Y,W,lo}$, which on average is around 30% lower:

$$\mu_{Y,W,lo} \approx 0.7 \times \mu_{Y,W} \tag{2.13}$$

In contrast to dry concrete (as also shown in Fig. 2.43) on asphalt and, in particular on wet and icy road surfaces, no further increase in the lateral cornering forces can be determined above $\alpha = 10°$ (i.e. $S_{Y,W} \approx 17\%$).

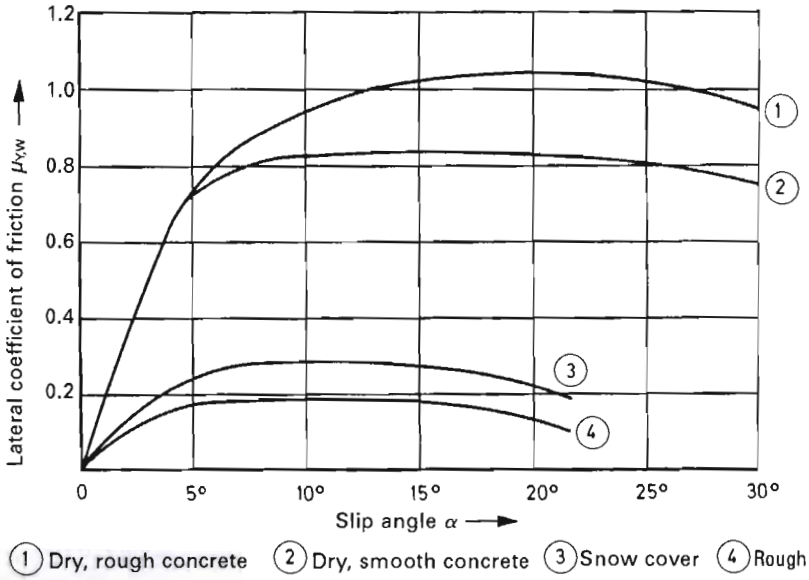

(1) Dry, rough concrete (2) Dry, smooth concrete (3) Snow cover (4) Rough ice cover

Fig. 2.43 Lateral coefficients of friction $\mu_{Y,W}$ as a function of slip angle and road condition, shown for an '82 series' summer tyre with around 90% deep profile. The ice temperature is around –4°C. The vertical force $F_{Z,W}$ was kept constant during the measurements to obtain the dimensionless values of $\mu_{Y,W}$. The maximum at $\alpha = 20°$ on a very skid-resistant road can be seen clearly. The further $\mu_{Y,W}$ sinks, the further it moves towards smaller angles.

2.8.4 Lateral cornering force properties on dry road

Figure 2.44 shows the usual way in which a measurement is carried out for a series 82 tyre. The lateral force appears as a function of the vertical force in kilonewtons and the slip angle α serves as a parameter. A second possibility can be seen in Fig. 2.45; here, for the corresponding series 70 tyre, $\mu_{Y,W} = F_{Y,W}/F_{Z,W}$ is plotted against α and $F_{Z,W}$ serves as a parameter. The degree of curvature of the graphs in both figures shows that slope at any point changes as a function of $F_{Z,W}$ or $\mu_{Y,W}$. The maximum occurs with large angles and small vertical forces. A less stressed tyre in relation to its load capacity therefore permits greater coefficients of friction and higher cornering speeds than one whose capacity is fully used.

This result, which has been used for a long time in racing and sports cars, has also become popular in modern cars, A mid-range standard car can be taken as an example. The car manufacturer specifies $p_T = 2.2$ bar/2.5 bar under full load for the front and rear wheels 185/65 R 15 88H. At these pressures, the load capacity, in accordance with Figs 2.13 and 2.15, is:

front 505 kg and rear 560 kg

Figure 5.10 contains the authorized axle loads from which the wheel load (divided by two) results:

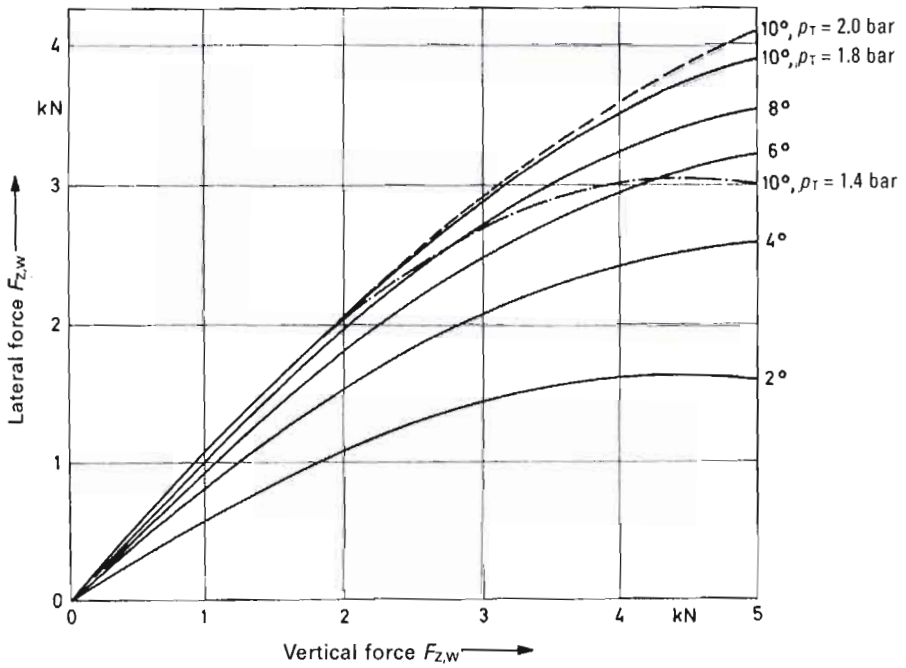

Fig. 2.44 Lateral cornering forces of the 155 R 13 78 S '82 series' steel radial tyre, measured on a dry drum at p_T = 1.8 bar. The load capacity at this pressure is around 360 kg, corresponding to a vertical force $F_{Z,W}$ = 3.53 kN. Also shown are the forces at α = 10° and P_T = 1.4 bar and 2.0 bar to indicate the influence of the tyre pressure on the lateral cornering properties.

front 375 kg and rear 425 kg

As described in Section 2.2.6, at speeds up to 210 km h^{-1} (H tyres), an increase in tyre pressure of 0.3 bar is necessary or there is only a correspondingly lower load capacity. This then is, with p_T = 1.9 bar at the front or 2.2 bar at the back,

450 kg and 505 kg

Thus, the actual load factor k_m at 210 km/h becomes:

$$\begin{aligned} &\text{front } k_{m,f} = (375/450) \times 100 = 83\% \\ &\text{back } k_{m,r} = (425/505) \times 100 = 84\% \end{aligned} \qquad (2.14)$$

2.8.5 Influencing variables

2.8.5.1 Cross-section ratio *H/W*

The 185/65 R 15 88H size used as an example in the previous section is a 65 series wide tyre; the 15″ diameter also allows a good sized brake disc diameter (Fig. 2.10).

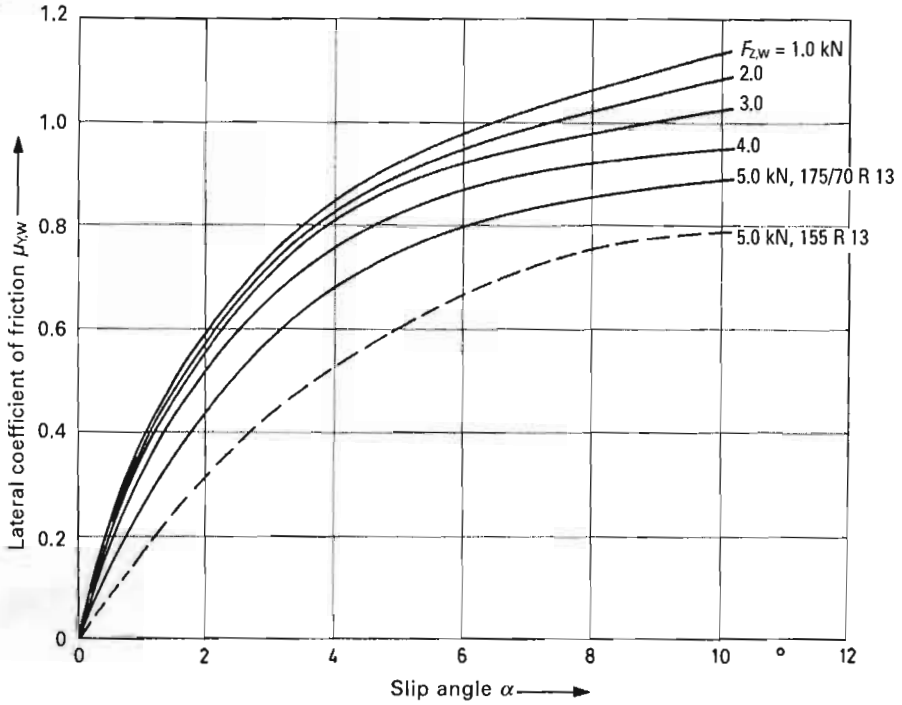

Fig. 2.45 Lateral coefficients of friction $\mu_{Y,W}$ as a function of the slip angle α and the vertical force $F_{Z,W}$, measured on a dry drum on a 175/70 R 13 82 S tyre at p_T = 2.0 bar. The tyre, which has been inflated in such a manner, carries 395 kg or $F_{Z,W}$ = 3.87 kN. In order to indicate the influence of the cross-section on the transferable lateral forces the 82 series 155 R 13 78 S tyre was also included.

In contrast to the 82 series standard tyre, the sizes of the 70 series and wide tyres (H/W = 0.65 and below) generate higher lateral cornering forces at the same slip angles (Figs 2.9, 2.45 and 2.46). As can be seen in Fig. 1.6, these, as $F_{Y,W,o} = \mu_{Y,W}\,(F_{Z,W} + \Delta F_{Z,W})$, are all the greater, the faster the vehicle takes a bend.

2.8.5.2 Road condition

The force transmission ratios between the tyres and road are determined by the state of the road (see construction, surface roughness and condition; Figs 2.43 and 2.47).

2.8.5.3 Track width change

The track width change that exists, in particular on independent wheel suspensions described in Section 3.3, causes undesirable lateral forces at the centres of tyre contact on both wheels when the vehicle is moving unimpeded in a straight line. Figures 3.5 and 3.6 show this, and also what lateral forces can occur if a series 82 radial tyre rolling in a straight line is brought out of its direction by an

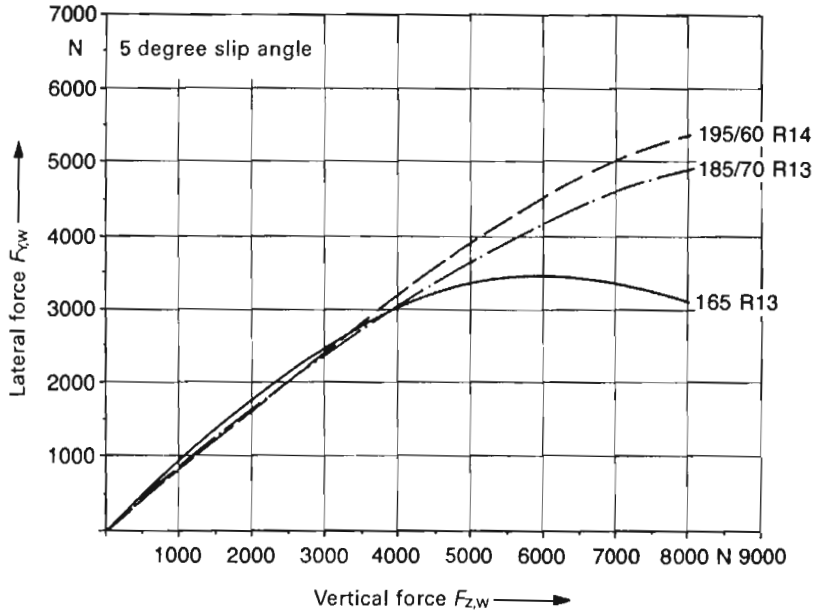

Fig. 2.46 Lateral force $F_{Y,W}$ dependent on vertical force $F_{Z,W}$ and tyre sizes of different *H/W* ratios: 165 R 13 82 H, 185/70 R 13 85 H and 195/60 R 14 85 H.
Up to $F_{Z,W}$ = 4000 N the curves are more or less the same, but at higher loads the more favourable lateral cornering properties of the wide tyre are evident.

suspension-kinematic dependent change. This effect is magnified by an increase in slip rigidity, as, for example, in wide tyres.

2.8.5.4 Variations in vertical force

During cornering, vertical force variations $\pm\Delta F_{Z,W}$ in the centre of tyre contact cause a reduction in the transferable lateral forces $F_{Y,W}$ as the tyre requires a certain amount of time and distance for the build-up of lateral forces. The loss of lateral force $\Delta F_{Y,W,4}$ depends on the effectiveness of the shock absorbers, the tyre pressure p_T (which can enhance the 'springing' of the wheels, see Equation 5.6) and the type of wheel suspension link mountings. Further influences are wheel load and driving speed. To calculate cornering behaviour, an average loss of lateral force $\Delta F_{Y,W,4}$ due to variations in vertical force and dependent only on tyre design and slip angle α, should be considered:

$$\Delta F_{Y,W,4} \approx 40 \text{ N per degree } \alpha \qquad (2.15)$$

2.8.5.5 Camber change

Wheels that incline with the body during cornering have a similar, detrimental influence on the transferability of lateral forces. As can be seen from Fig. 1.6, positive angle ($+\varepsilon_w$) camber changes occur on the outside of the bend and negative

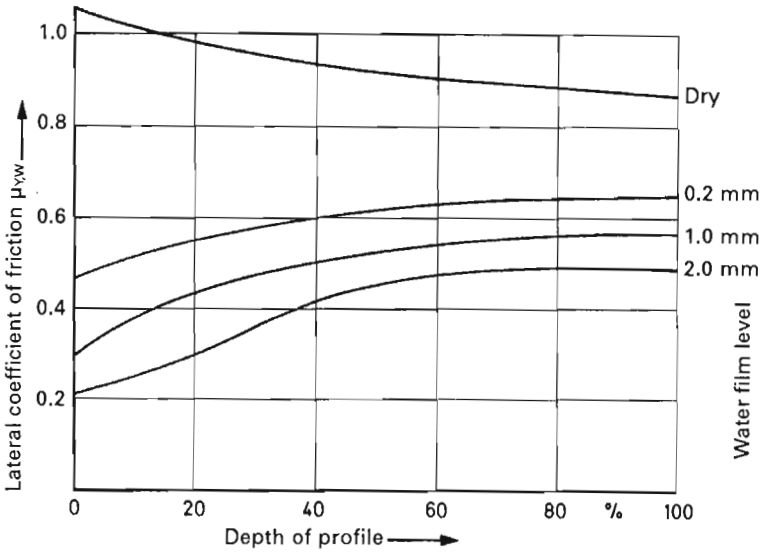

Fig. 2.47 Possible lateral friction coefficients $\mu_{Y,W}$ of a steel radial tyre 155 R 13 78 S depending on the depth of the tyre profile as a percentage (starting from 8 mm = 100%) at p_T = 1.8 bar, α = 10°, v = 60 km/h and varying water film levels in mm.

The improved grip of the treadless tyre on a dry road can be seen clearly as can its significantly poorer grip in the wet; a fact which also applies to the coefficient of friction in the longitudinal direction (see Section 2.7.2).

angles ($-E_W$)on the inside of the bend as a consequence of the body roll. The lateral forces are directed to the centre point of the bend (Fig. 3.13). If a wheel is 'cambered' against this, in other words inclined at the top towards the outside of the bend, the possibility of transferring lateral forces reduces; on a dry road surface, depending on the tyre size, the change is

$$\Delta F_{Y,W,3} = 40 \text{ N to } 70 \text{ N per degree of camber} \qquad (2.16)$$

To counteract this, a greater slip angle must occur and greater steering input becomes necessary for the front wheels. This makes the vehicle understeer more (Fig. 2.41) and appear less easy to handle. Furthermore, the steering aligning moment (see Section 3.10.3) also increases. If this effect occurs on the rear axles – as is the case with longitudinal link axles (Fig. 1.14) – the vehicle has a tendency to oversteer. Negative camber $-\varepsilon_W$ on the outside of the bend and positive $+\varepsilon_W$ on the inside would have exactly the opposite effect. Wheels set in this manner would increase the lateral forces that can be absorbed by the amount stated previously for $\Delta F_{Y,W,3}$ and cause a reduction in the tyre slip angle.

2.8.5.6 Lateral force due to camber

Wheels according to the body roll inclined towards the outside edge of the bend (Fig. 1.6) try to roll outwards against the steering direction, so that additional

camber forces are required in the tyre contact patches to force the wheels in the desired steering direction. As these camber forces act in the same direction as the centrifugal force $F_{c,Bo\ or\ v}$ in the case described, greater lateral slip forces $F_{Y,W,f,o}$, $F_{Y,W,f,i}$, $F_{Y,W,r,o}$ and $F_{Y,W,r,i}$ and hence greater slip angles must be applied to maintain the balance of forces on the part of the tyres.

The average force F_{ε_W} with the standard camber values for individual wheel suspensions on a dry road are (see Section 2.2.3 in Ref. 9):

$$F_{\varepsilon_W} \approx F_{Z,W} \times \sin \varepsilon_W \tag{2.17}$$

2.9 Resulting force coefficient

Rolling resistance increases when negotiating a bend (see Equation 2.4a), and the vehicle would decelerate if an increased traction force $F_{X,W,A}$ did not create the equilibrium needed to retain the cornering speed selected. In accordance with Equation 6.36, $F_{X,W,A}$ is dependent on a series of factors and the type of drive system (front- or rear-wheel drive); on single-axle drive (see Sections 1.4 to 1.6), the traction force on the ground stresses the force coefficient of friction (the coefficient of)

$$\mu_{X,W} = F_{X,W,A,f\ or\ r}/F_{Z,V,f\ or\ r} \tag{2.15}$$

and thus greater slip angles at the driven wheels. With given values for cornering speed and radius (see Equation 2.8) the resulting force coefficient μ_{rsl} can be determined:

$$\mu_{rsl} = (\mu_{Y,W}^2 + \mu_{X,W}^2)^{\frac{1}{2}} \tag{2.18}$$

μ_{rsl} cannot be exceeded because the level depends on the road's surface and the condition.

When braking on a bend, additional longitudinal forces $F_{X,W,b}$ occur on all wheels (see Section 6.3.1), and act against the direction of travel. In this case Equation 2.18 also applies.

On standard vehicles and front-wheel drives, the front wheels take 70–80% of the braking force and the rear wheels only 20–30%. This means that the slip angles increase on both axles, but more at the front than the rear and the vehicle tends to understeer (Fig. 2.41 and Equation 6.20). If the wheels of an axle lock, the friction becomes sliding friction and the vehicle pushes with this pair of wheels towards the outside of the bend (Figs 6.8 to 6.10).

Taking into consideration the maximum possible values in the longitudinal and lateral direction of the road – known respectively as $\mu_{X,W,max}$ and $\mu_{X,W,min}$ – the increasing force coefficient can be calculated:

$$\mu_{X,W} = \mu_{X,W,max}\left[1 - \left(\frac{\mu_{Y,W}}{\mu_{Y,W,max}}\right)^2\right]^{\frac{1}{2}} \tag{2.19}$$

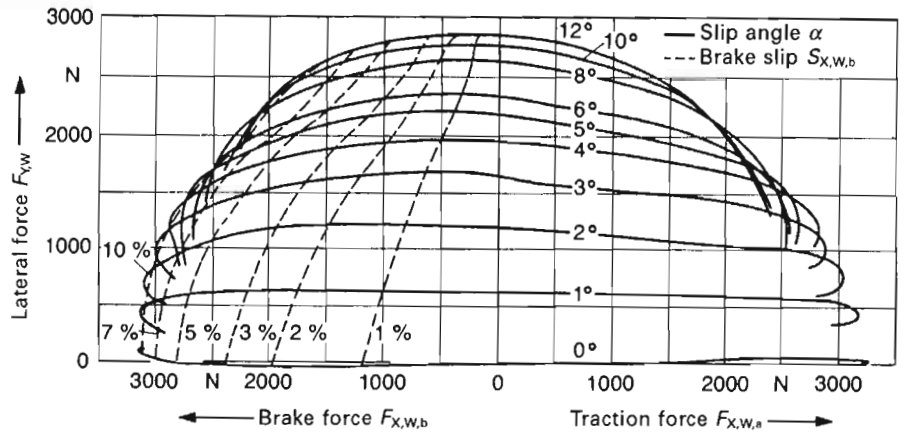

Fig. 2.48 Tyre-tangential lateral force performance characteristics with slip angles and brake slip as parameters. The study was carried out on a 18565 R 14 86 S radial tyre loaded at 300 kg at p_T = 1.5 bar. The shape of the curves indicates that, with increasing longitudinal forces, those which can be absorbed laterally reduce. At 1.5 bar, the tyre carries a weight of 350 kg, i.e. it is only operating at 86% capacity.

Consider as an example a braking process on a dry road at 100 km/h on a bend with R = 156 m. Using Equation 2.9 the calculation gives $\mu_{Y,W}$ = 0.5.

Figure 2.48 shows a measurement on the tyre in question where the greatest coefficient of friction in the lateral direction at $F_{Z,W}$ = 2490 N, ε_W = 10% and α = 4° (see Equation 2.11) amounts to

$$\mu_{Y,W,max} = F_{Y,W}/F_{Z,W} = 2850/2940 \text{ (N/N)} \qquad \mu_{Y,W,max} = 0.97$$

In the longitudinal direction the possible braking force $F_{X,W,b}$ = 3130 N is at α = 0° and therefore (see Equation 2.5),

$$\mu_{X,W,max} = F_{X,W,b}/F_{Z,W} = 3130/2940 \text{ (N/N)}$$
$$= 1.06$$

and

$$\mu_{X,W} = 1.06\left[1 - \left(\frac{0.5}{0.97}\right)^2\right]^{\frac{1}{2}}$$
$$= 0.91$$

The lateral forces that the tyre can absorb during braking can also be calculated:

$$\mu_{Y,W} = \mu_{Y,W,max}\left[1 - \left(\frac{\mu_{X,W}}{\mu_{X,W,max}}\right)^2\right]^{\frac{1}{2}} \qquad (2.19a)$$

$\mu_{X,W} = 0.7$ should be given. The lateral force coefficient (which can be used) is:

$$\mu_{Y,W} = 0.97\left[1 - \left(\frac{0.7}{1.06}\right)^2\right]^{\frac{1}{2}}$$
$$= 0.73$$

At $S_{X,W,b} = 10\%$ and $\alpha = 4°$ the transferable lateral force is

$$F_{Y,W} = \mu_{Y,W} \times F_{Z,W} = 0.73 \times 2940$$
$$= 2146 \text{ N}$$

and the available braking force is

$$F_{X,W,b} = \mu_{X,W} \times F_{Z,W} = 0.7 \times 2940$$
$$= 2058 \text{ N}$$

2.10 Tyre self-aligning torque and caster offset

2.10.1 Tyre self-aligning torque in general

The focal point of the force of the tyre contact patch lies behind the middle of the wheel because of its load- and lateral-force-related deformation. As a result, the point of application of the lateral force alters by the amount $r_{\tau,T}$, known as the caster offset, and comes to lie behind the centre of the wheel (Fig. 3.119). On the front wheels, the lateral cornering force $F_{Y,W,f}$ together with $r_{\tau,T}$ (as the force lever) gives the self-aligning moment $M_{Z,T,Y}$ which superimposes the kinematic alignment torque and seeks to bring the input wheels back to a straight position (Section 3.8).

The self-aligning torque, lateral force and slip angle are measured in one process on the test rig. $M_{Z,T,Y}$ is plotted as a function of the slip angle (Fig. 2.49), the vertical force $F_{Z,W}$ serves as a parameter. The higher $F_{Z,W}$, the greater the self-alignment and, just like the lateral force, the moment increases to a maximum and then falls again. $M_{Z,T,Y,max}$ is, however, already at $\alpha \approx 4°$ (as can be seen in Fig. 2.43) and not, on a dry road, at $\alpha \geqslant 10°$.

2.10.2 Caster offset

Caster offset, $r_{\tau,T}$, is included in practically all calculations of the self-aligning moment during cornering (see Section 3.10.3). The length of this can easily be calculated from the lateral force and moment:

$$r_{\tau,T} = M_{Z,T,Y}/F_{Y,W} \text{ (m)} \qquad (2.20)$$

This requires two images, one which represents $F_{Y,W} = f(F_{Z,W}$ and $\alpha)$ or $\mu_{Y,W} = f(F_{Z,W}$ and $\alpha)$, and another with $M_{Z,T,Y} = f(F_{Z,W}$ and $\alpha)$. The values of the 175/70R

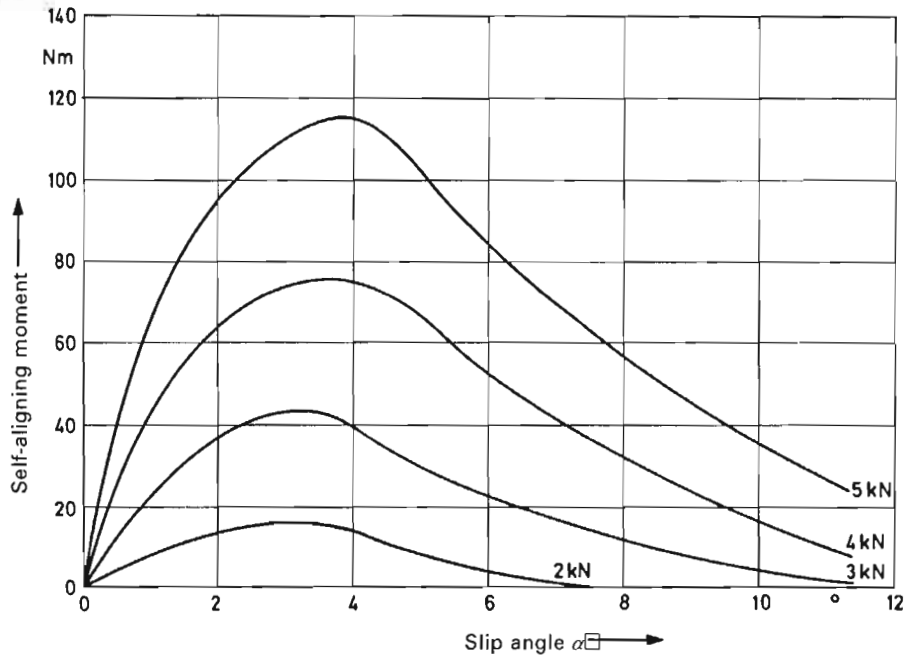

Fig. 2.49 Self-aligning torques of a 175/70 R 13 82 S steel radial tyre measured on a dry drum as a function of the slip angle at p_I = 2.0 bar. The vertical force $F_{Z,W}$ in kilonewtons is used as a parameter. The torques increase sharply at low angles, reach a maximum at α = 3° to 4° and then reduce slowly. As the cornering speed increases, the tyre self-aligning torque decreases, while the kinematically determined torque increases (see Section 3.8).

13 82 S steel radial tyre shown in Figs 2.45 and 2.49 and measured at p_T = 2.0 bar serve as an example. At α = 2° and $F_{Z,W}$ = 5.0 kN the coefficient of friction $\mu_{Y,W}$ = 0.44 and therefore:

$$F_{Y,W} = \mu_{Y,W} \times F_{Z,W} = 0.44 \times 5.0 = 2.2 \text{ kN}$$
$$= 2200 \text{ N}$$

At the same angle and with the same wheel force, the self-aligning torque is $M_{Z,T,Y}$ = 95 Nm and therefore

$$r_{\tau,T} = M_{Z,T,Y}/F_{Y,W} = 95/2200 = 0.043 \text{ m}$$
$$= 43 \text{ mm}$$

Figure 2.50 shows the caster (caster offset trail) calculated in this manner. Higher lateral forces necessitate greater slip angles, and the latter result in smaller self-aligning moments and a reduced caster offset. The explanation for this fact is that, at low slip angles, only the tyre profile is deformed at the area

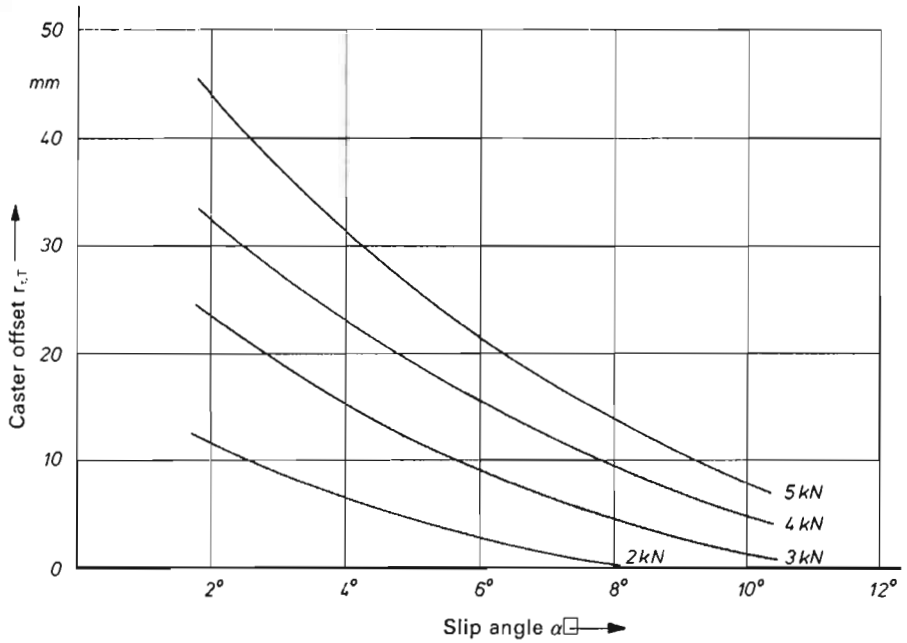

Fig. 2.50 Caster offset of tyre $r_{\tau,T}$ calculated from Figs 2.45 and 2.49 for 175/70 R 13 82 S steel radial tyres at p_T = 2.0 bar. The higher the vertical force $F_{Z,W}$ (in kN) and the smaller the angle α, the longer is $r_{\tau,T}$.

of contact. The point of application of the lateral force can therefore move further back, unlike large angles where, principally, the carcass is deformed. High vertical wheel forces cause the tyre to be severely compressed and therefore an increase both in the area of tyre contact and also in the caster offset occur.

2.10.3 Influences on the front wheels

The tyre self-aligning torque is one of the causes for the steering forces during cornering; its level depends on various factors.

2.10.3.1 Dry roads

The self-aligning torque is usually measured on a roller test bench with the drum allowing a coefficient of friction of μ_0 = 0.8 to 0.9 between its surface and the tyre. If the resultant self-aligning torque on the open road is required, it is possible to approximate the value $M_{Z,T,Y,\mu}$ using a correction factor:

$$k_\mu = \mu_{Y,W}/\mu_0 \tag{2.21}$$

A cement block with $\mu_{Y,W} \sim 1.05$ (Fig. 2.43) and the 175/70 R 13 82 S radial tyre can be used as an example. In accordance with Fig. 2.49,

$M_{Z,T,Y}$ = 40 N m with $F_{Z,W}$ = 3 kN and α = 4°

As a correction factor this gives

$$k_\mu = \mu \frac{\text{road}}{\text{roller}} = \frac{\mu_{Y,W}}{\mu_0} = \frac{1.05}{0.80}$$
$$= 1.31$$

and thus

$$M_{Z,T,Y,\mu} = k_\mu \times M_{Z,T,Y} = 1.31 \times 40$$
$$= 52.4 \text{ N m}$$

2.10.3.2 Wet roads

Provided that k_μ is independent of tyre construction and profile, the approximate value for a wet road can also be determined. In accordance with Fig. 2.47, with 1 mm of water on the surface and full profile depth the $\mu_{Y,W}$ value reduces from 0.86 to 0.55. Owing to the reduced coefficient of friction, only a smaller value $M_{Z,T,Y,\mu}$, can be assumed; in other words,

$$k_\mu = \mu_{Y,W} \frac{\text{wet}}{\text{roller}} = \frac{0.55}{0.86} = 0.64, \text{ and}$$

$$M_{Z,T,Y,\mu} = 0.64 \times 40 \text{ Nm}$$
$$= 25.6 \text{ Nm}$$

A greater water film thickness may cause the coefficient of friction to reduce but the self-aligning moment increases and the water turns the wheel back into the straight position. Furthermore, the self-aligning maximum shifts towards smaller slip angles when the road is wet.

2.10.3.3 Icy roads

Only with greater vertical forces and small slip angles is the smoothness of the ice able to deform the area of tyre contact and generate an extremely small moment, which is nevertheless sufficient to align the tyre. Low front axle loads or greater angles α arising as a result of steering corrections would result in a negative moment $-M_{Z,T,Y}$ (in other words in a 'further steering input' of the tyres). The wheel loads at the front, which were only low, were already a problem on rear-engine passenger vehicles.

2.10.3.4 Longitudinal forces

As shown in Fig. 3.119, traction forces increase the self-aligning torque; the equation for one wheel is

$$M_{Z,W,a} = F_{Y,W} \cdot r_{\tau,T} + F_{X,W,a} \cdot r_T = F_{z,W} (\mu_{Y,W} \cdot r_{\tau,T} + \mu_{X,W} \cdot r_T) \quad (2.22)$$

During braking the moment fades and reduces to such an extent that it even becomes negative and seeks to input the wheels further. The formula for one wheel is

$$M_{Z,W,b} = F_{Y,W} \cdot r_{\tau,T} - F_{X,W,b} \cdot r_T$$
$$= F_{Z,W} (\mu_{Y,W} \cdot r_{\tau,T} - \mu_{X,W} \cdot r_T) \quad (2.23)$$

The length of the paths $r_{\tau,T}$ and r_T can be found in the details of Fig. 3.117.

2.10.3.5 Tyre pressure

When the tyre pressure is increased the self-aligning torque reduces by 6–8% per 0.1 bar, and increases accordingly when the pressure reduces, by 9–12% per 0.1 bar.

A reduction in pressure of, for example, 0.5 bar could thus result in over a 50% increase in the moment, a value which the driver would actually be able to feel.

2.10.3.6 Further influences

The following have only a slight influence:

- positive camber values increase the torque slightly, whereas negative ones reduce it;
- $M_{Z,T,Y}$ falls as speeds increase because the centrifugal force tensions the steel belt which becomes more difficult to deform (Fig. 2.16);
- widening the wheel rim width slightly reduces self-alignment.

2.11 Tyre overturning moment and displacement of point of application of force

A tyre which runs subject to lateral forces on the tyre contact patch is subject to deformation; there is a lateral displacement between the point of application of the normal force (wheel load; Fig. 3.119) and the centre plane of the wheel. Figure 2.51 shows the lateral drift of the normal (wheel load) point of application which is dependent on the size of the tyre, the lateral force and the camber angle and to a large extent on the construction of the tyre. Low section tyres with a small height-to-width ratio and a high level of sidewall rigidity exhibit greater lateral displacement. The rollover resistance of the vehicle is considerably reduced, as there is a decrease in the distance between the point of contact of the wheel and the centre of gravity of the vehicle.

This displacement results in the emergence of tyre overturning moments $M_{X,T,\alpha}$ about the longitudinal axis of the tyre (Fig. 2.52).

Both the lateral displacement of the point of application of the normal force and the tyre overturning moments must be taken into account when considering the overturning behaviour of vehicles, as they can considerably reduce rollover resistance, if, for example, a vehicle has a high centre of gravity and a small track dimension.

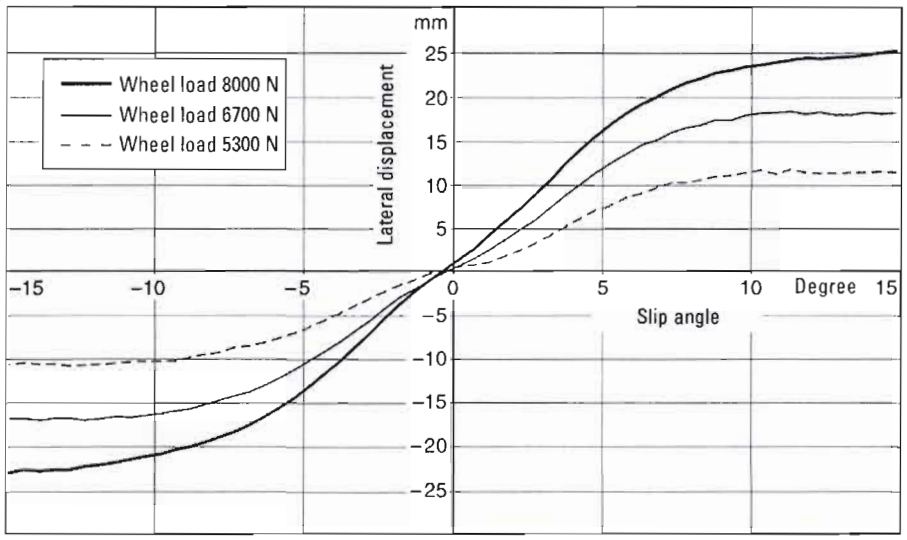

Fig. 2.51 Lateral displacement of normal (wheel load) point of application depending on slip angle and wheel load; measurements by Continental on a tyre of type 205/65 R 15 94 V ContiEcoContact CP.

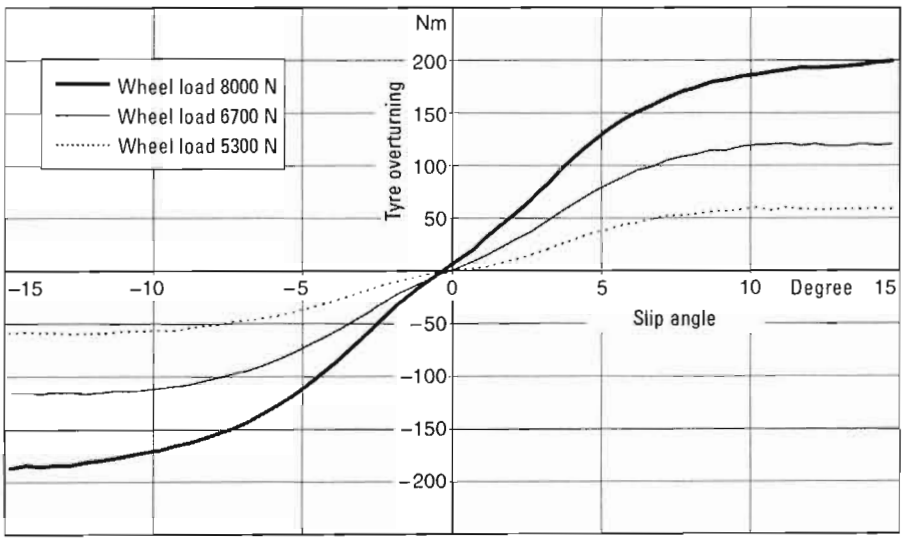

Fig. 2.52 Tyre overturning moments $M_{x,T,\alpha}$ on the wheel as a result of the build-up of lateral forces at different slip angles and wheel loads $F_{z,w}$; measurements by Continental on a tyre of type 205/65 R 15 94 V ContiEcoContact CP.

2.12 Torque steer effects

Torque steer effects, i.e. changes in longitudinal forces during cornering, are an important criterion for the definition of transient handling characteristics. The torque steer effects depend on the size of the change in the longitudinal force, the adherence potential between the tyres and the road, the tyres and the kinematic and elastokinematic chassis design.

2.12.1 Torque steer effects as a result of changes in normal force

Torque steer effects usually occur during cornering when a driver has to slow down on a wrongly assessed bend by reducing the amount of acceleration or applying the brake.

The reaction force acting at the centre of gravity of the vehicle causes an increase in front axle load with a simultaneous reduction in the load on the rear axle. At an initially unchanged slip angle, the distribution of lateral forces changes as a result. If the force coefficient relating to the simultaneous transfer of longitudinal and transverse forces is sufficient, e.g. in the case of torque steer effects owing to reduction in acceleration or gentle braking (cf. Fig. 2.48), the increased lateral force corresponding to the increase in normal force on the front axle results in a yawing moment which allows the vehicle to turn into the bend.

If the adhesion potential is exceeded as a result of fierce braking or a low force coefficient, the tyres are no longer able to build up the necessary lateral forces. This results in an over- or understeering vehicle response depending on the specific case, be it a loss of lateral force on the front axle or rear axle or both.

2.12.2 Torque steer effects resulting from tyre aligning torque

The lateral displacement of the tyre contact area as a result of lateral forces leads to longitudinal forces being applied outside the centre plane of the wheel (Fig. 2.53).

This effect causes an increase in tyre aligning torque in driven wheels. In rear-wheel drive vehicles, this torque has an understeering effect with tractive forces, whereas it has an oversteering effect where there is a change in braking power.

In front-wheel drive vehicles, the resultant tractive force vector applies about lever arm $l_f \times \sin \delta_f$ offset from the centre of gravity of the vehicle (Fig. 2.54), so that an oversteering yawing moment is produced during driving which alters with application of a braking force to a (small) understeering yawing moment.

2.12.3 Effect of kinematics and elastokinematics

An attempt is made to keep the torque steer effects of a vehicle low by means of specific chassis design. The above-mentioned changes in forces produce

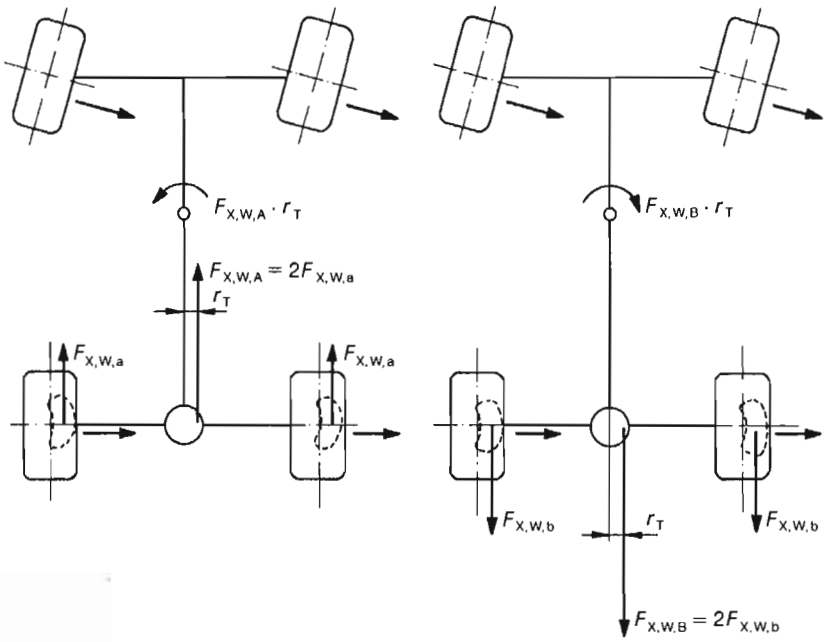

Fig. 2.53 The deformation of the tyre contact area during cornering results in aligning torque of the lateral forces which is further intensified by tractive forces and produces an understeering yawing moment. If there is a change in load, the braking forces produce an oversteering yawing moment.

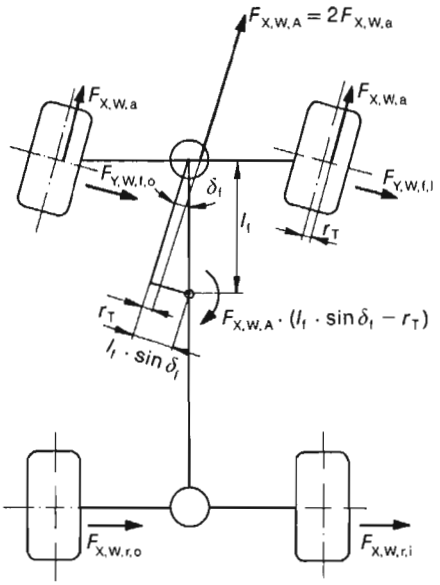

Fig. 2.54 With front-wheel drive, an oversteering yawing moment is produced, because the resultant tractive force vector is applied about lever arm $l_f \times \sin \delta_f$ displaced to the centre of gravity of the vehicle.

bump and rebound travel movements on the axles. The results, depending on the design of the chassis, in kinematic and elastokinematic toe-in and camber changes which can be used to compensate for unwanted changes in lateral forces, particularly in the case of multi-link suspensions. With unfavourable axle design and construction, there is, however, also the possibility of an increase in the torque steer effects.